HIGH TEMPERATURE GAS COOLED REACTOR FUEL FAILURE IN THE ABSENCE OF CORE COOLING

A Thesis

Submitted to the Graduate Faculty of the
Louisiana State University and
Agricultural and Mechanical College
in partial fulfillment of the
requirements for the degree of
Master of Science

in

The Department of Nuclear Engineering

by
Farzad Rahnema
B.S., Illinois Institute of Technology, 1974
May, 1977

Dedicated to

my father Javad, my mother Robab, and

my wife Mahnaz

ACKNOWLEDGMENT

The author wishes to express his sincere appreciation to the members of his examining committee for their assistance in the preparation of this thesis. Special recognition is due his major professor, Dr. R. E. Miles, for his continual guidance, encouragement, and contribution of useful computer codes. His advice and profound insight have been invaluable throughout all phases of this work.

The author is grateful to General Atomic Company for providing the information on high temperature gas cooled reactor fuel failure rates.

The author is deeply indebted to his wife, Mahnaz, for her devoted encouragement, understanding, and patience.

Sincere thanks are given to the author's parents, Robab and Javad, for their emotional and financial support throughout his university career. Their faith and confidence in him has been an inspiration in his studies.

TABLE OF CONTENTS

TABLE OF CONTENTS (CONTINUED)

LIST OF TABLES

LIST OF FIGURES

ABSTRACT

Nuclear power plants are studied intensively at all phases of development and considerable attention is directed toward containment of fission products during hypothetical failure sequences. For a high temperature gas cooled reactor, the primary containment barrier is the coating on individual fuel particles, which would be expected to fail if subjected to extreme temperatures. Fission product heating, following a design basis depressurization accident and auxiliary circulators failure, may lead to such temperature extremes and result in a fission product release. The probability of fuel particle failure is related to pre-accident irradiation history as well as post-accident temperatures. Although a number of different models with varying degrees of accuracy can be used to assess the temperature response of the core, this thesis focused on insights to the problem of fuel failure that can be gained by use of a homogeneous adiabatic heat transfer model. This conservative model assumed a homogeneous distribution of fission products and no heat transfer from the reactor core. As a typical case, the General Atomic 1160 megawatt electrical reactor was analyzed for temperature-excursion failure for the temperature range of 1600 to 2000 degrees Centigrade. Equations were derived for the reactor temperature rise from heat released by fission product decay. These mathematical equations were reduced to simple polynomial approximations to simplify calculations. The polynomial approximations were coupled with empirical expressions for fuel failure percentages as a function of

temperature and burnup, F(T,BU), based on out-of-pile annealing experiments. For the simplest linear-approximation, the fuel failure as a function of time is given by

$$F(t,BU) \simeq \frac{100}{131 + 3.45\ BU}\ [(6.098\ t + 1038) - 1869 + 3.45\ BU],$$

in which t is the time in minutes following the design basis depressurization accident, and BU is the pre-accident percentage burnup. Using the most accurate calculation, even for a burnup prior to refueling after four years of reactor operation (worst case) no fuel failure would occur before 93 minutes, and even with less than 20% burnup all fuel would fail at 158 minutes.

Chapter I

INTRODUCTION

Evaluation of the safety of a nuclear power plant is accomplished, in part, by analyses made of the response of the plant to postulated malfunctions or failures of equipment. Therefore, a correct analysis of a Hypothetical Fission Product Release, HFPR, in a large High Temperature Gas Cooled Reactor, HTGR, has an important impact on design specifications for components and systems from the standpoint of public health and safety, and licensability of the plant.

This thesis represents a study of fuel failure, which can lead to release of fission products in the reactor core, as a function of time following a design basis depressurization accident, DBDA, in the HTGR.

HTGR Evolution

The current HTGR evolved from stations in operation or under construction in Europe and the USA. The 40 megawatt electrical, MW(e), Peach Bottom Nuclear Power Plant[1] was the first HTGR in the U.S. constructed by the Bechtel Company and operated by Philadelphia Electric Company. General Atomic was responsible for the nuclear steam supply system. Criticality was achieved in March 1966. In early 1970 after generating 4.7×10^8 kilowatt hour, kwh, of electricity with a burnup of 30,000 megawatt day per metric ton,

MWD/MT, the first core was replaced. The second core which was designed for a three year life (about 900 effective full power days) and a burnup of 73,000 MWD/MT was shutdown in Spring of 1974.

Fort St. Vrain[2], with a power level of 330 MW(e), is the second HTGR constructed in the U.S. with General Atomic as the major contractor. Fort St. Vrain was built for the Public Service Company of Colorado.

Because of the technology and operating experience gained with the first two HTGR's in the U.S., General Atomic was able to design larger HTGR plants. These plants were commercially offered between 1971 and 1974. However, because of cost escalation and economic problems they have been temporarily removed from the commercial market. Some important characteristics of these plants are shown in Table 1.1.

Description of HTGR Fuel

The fuel element in the HTGR is made of a hexagonal block of graphite with fuel channels drilled blind from the top face[4]. The channels are filled with rods containing fuel particles, up to 60% by volume, bonded together with graphite matrix. The fuel channels are distributed in a triangular array with an ideal ratio of two fuel holes for each coolant channel drilled through the fuel element. A standard large HTGR fuel element assembly is shown in Figure 1.1. A standard fuel element into which control rods are inserted is shown in Figure 1.2.

Table 1.1

COMPARISON OF HTGR CHARACTERISTICS[3]

	Peach Bottom	Fort St. Vrain	770 MW	1160 MW	1540 MW
Power level					
MW(t)	115	842	2,000	3,000	4,000
MW(e)	40	330	770	1,160	1,540
Efficiency (%)	35	39	39	39	39
Inlet gas temperature (°C)	340	405	320	320	320
Outlet gas temperature (°C)	715	780	740	740	740
Average power density (W/cm^3)	8.3	6.3	8.2	8.4	8.2
Core configuration					
Active height (m)	2.28	4.75	6.34	6.34	6.34
Equivalent diameter (m)	2.79	5.94	7.07	8.47	9.88
Number of control rods	36	37 pairs	49 pairs	73 pairs	97 pairs
Fuel management					
Fuel lifetime at 80% capacity factor (yr)	3	6	4	4	4
Refueling cycle (yr)	3	1	1	1	1
Fraction of core replaced each cycle	1	1/6	1/4	1/4	1/4
Number of refueling regions	1	37	55	85	109
Fuel elements					
Number of elements	804	1,482	2,744	3,944	5,394
Number of columns	--	247	343	493	673
Elements per column	--	6	8	8	8
Basic fuel component	Particles in a graphite compact within a cylindrical purged sleeve	Bonded rods of particles within a hexagonal graphite element	Bonded rods of particles within a hexagonal graphite element	Bonded rods of particles within a hexagonal graphite element	Bonded rods of particles within a hexagonal graphite element
Element height (cm)	366	79.3	79.3	79.3	79.3
Element width (cm)	8.9	35.9 (across flats	35.9 (across flats)	35.9 (across flats)	35.9
Fuel exposure					
Average MWD/MT	73,000	100,000	95,000	95,000	95,000
Peak fast fluence (10^{21} nvt)	4.5	8	8	8	8

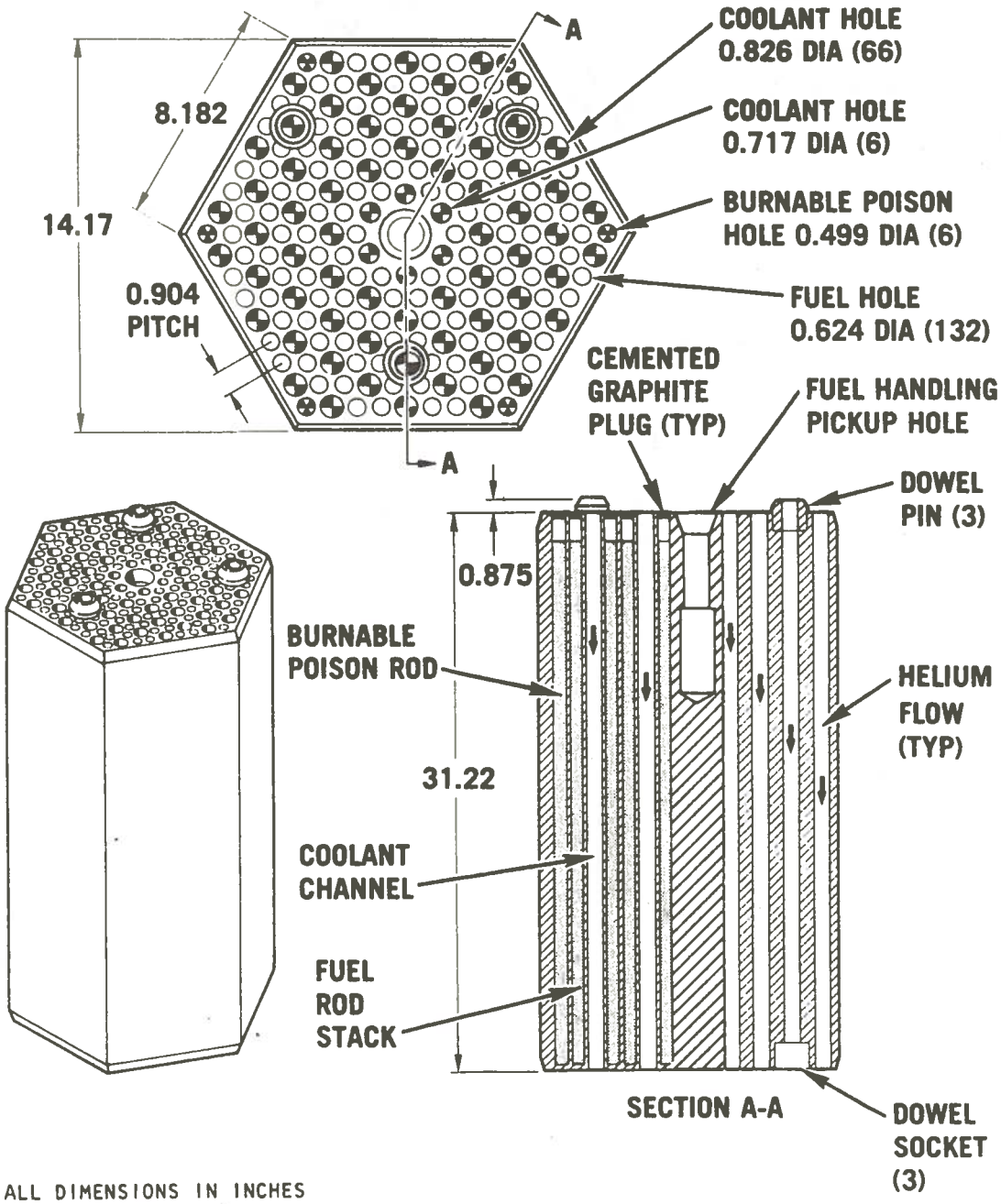

Figure 1.1. Standard LHTGR fuel element assembly [4]

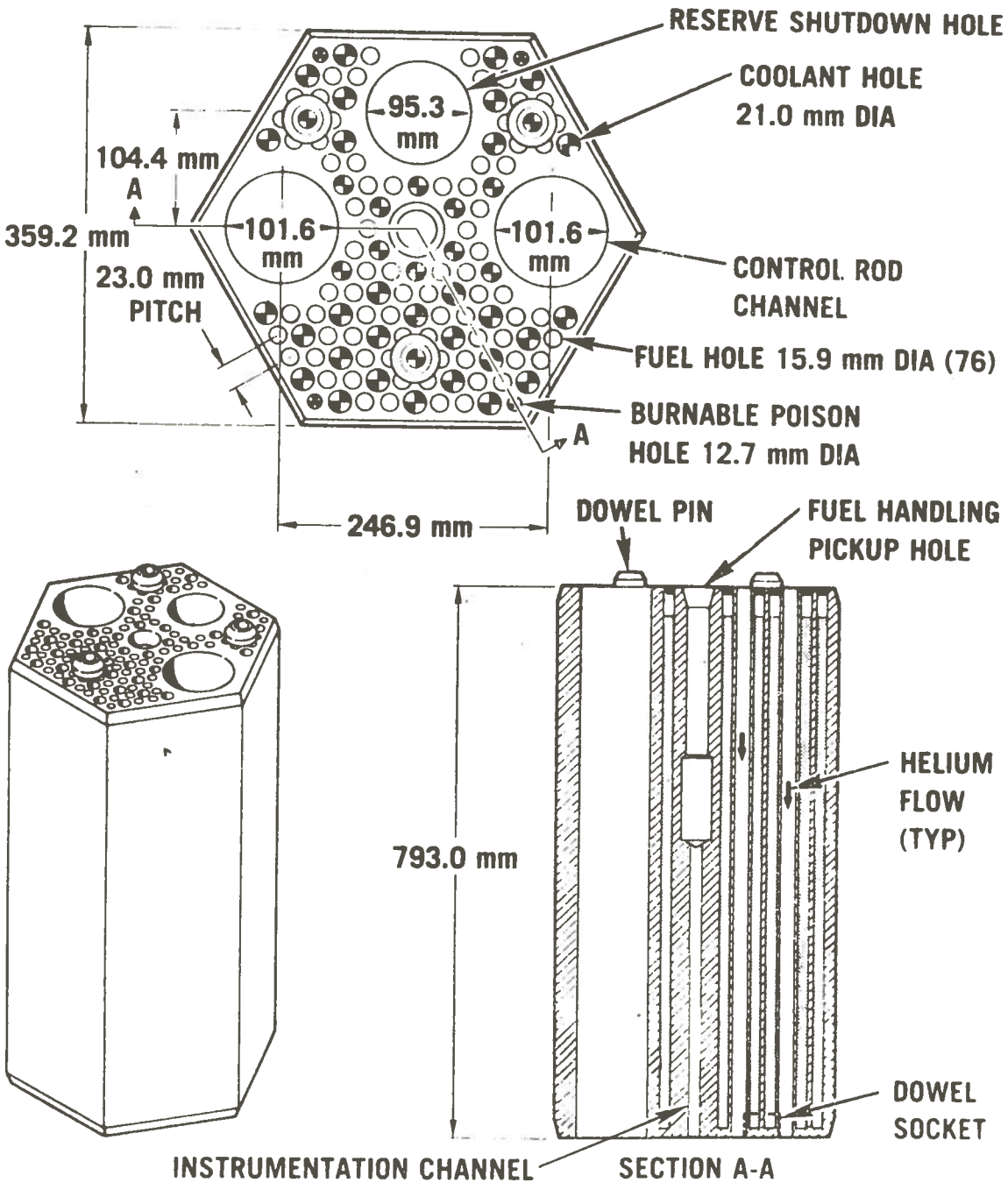

Figure 1.2. HTGR control fuel element[3]

Description of HTGR Fuel Particles

The HTGR uses two types of fuel particles, TRISO and BISO[4]. TRISO and BISO are acronyms representing a type of coating. The fissile material, UC_2, is surrounded by a low-density pyrolytic carbon (PyC) which acts as a buffer, a SiC layer, and a high-density isotropic pyrolytic carbon to retain fission products. The fertile material, ThO_2, is contained by a low-density pyrolytic carbon buffer and high-density isotropic pyrolytic carbon which acts as a pressure vessel to bound fission products. The HTGR fissile and fertile fuel particles are shown in Figure 1.3.

Under extreme operating conditions, the high-density outer PyC layer of a BISO coating or PyC-SiC-PyC sandwich of TRISO coating may rupture due to high internal fission gas pressure or coating stresses. This type of coating failure would lead to release of fission products. Design fuel kernel and coating properties, and purposes of the layers in TRISO and BISO coatings are given in Table 1.2 and 1.3 respectively.

HTGR Core Configuration

Fort St. Vrain reactor core has 247 columns of fuel elements with six elements in each column[3]. The 770 MW(e) HTGR contains 343 columns and each column has eight elements. The 1160 MW(e) plant consists of 493 columns, each having eight elements. The 1540 MW(e) HTGR contains 673 columns and each column has eight elements. The core configuration for the 1160 MW(e) HTGR is shown in Figure 1.4.

The columns of fuel elements are arranged in groups of seven for refueling purposes. Each of these groups which is called a

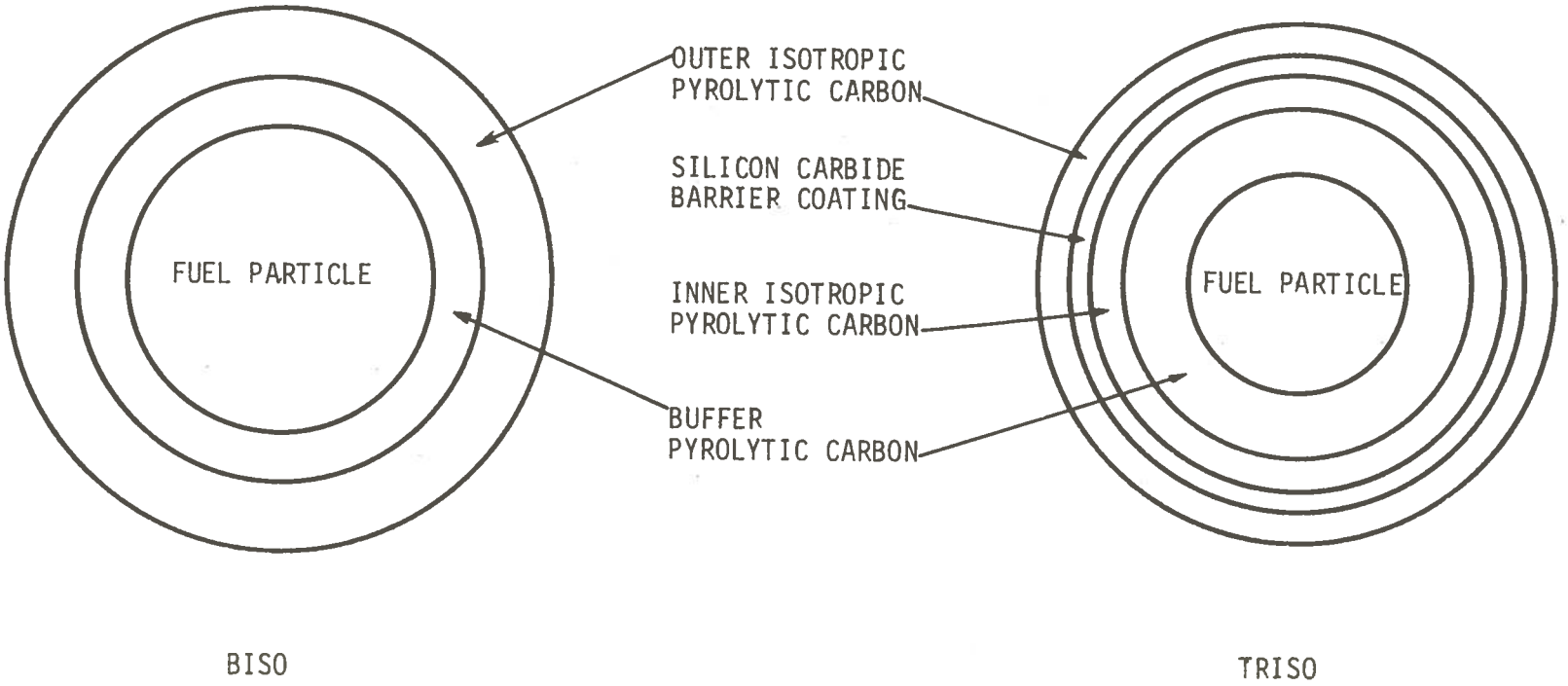

Figure 1.3. GA coated particles

Table 1.2

LARGE HTGR FUEL PARTICLE COATING DESIGNS[5]

	TRISO Fissile	BISO Fertile
Kernel		
Type	UC_2	ThO_2
Diameter (μm)	200	500
Density (g/cm^3)	≥10.3	≥9.5
Buffer		
Thickness (μm)	100	85
Density (g/cm^3)	1.10	1.10
Inner PyC		
Thickness (μm)	25	--
Density (g/cm^3)	1.90	--
OPTAF	≤1.25	--
SiC		
Thickness (μm)	25	--
Density (g/cm^3)	>3.18	--
Outer PyC		
Thickness (μm)	35	75
Density (g/cm^3)	1.80	1.85
OPTAF	≤1.20	≤1.20

Table 1.3

PURPOSE OF THE LAYERS IN TRISO AND BISO COATINGS (5)

	COATING LAYER	PURPOSE
BISO	BUFFER	• ATTENUATE FISSION RECOILS • PROVIDE VOID VOLUME FOR GASEOUS FISSION PRODUCTS AND FUEL SWELLING
BISO	ISOTROPIC PyC	• ACT AS A PRESSURE VESSEL TO CONTAIN GASEOUS FISSION PRODUCTS
TRISO	BUFFER	• ATTENUATE FISSION RECOILS • PROVIDE VOID VOLUME FOR GASEOUS FISSION PRODUCTS AND FUEL SWELLING
TRISO	INNER ISOTROPIC PyC	• PROTECT THE SiC LAYER FROM DETRIMENTAL REACTIONS WITH FUEL AND FISSION PRODUCTS
TRISO	SiC	• PROVIDE FISSILE-FERTILE SEPARATION CAPABILITY • PROVIDE MECHANICAL SUPPORT FOR THE PARTICLE • PROVIDE STRUCTURAL RIGIDITY AND DIMENSIONAL STABILITY • PROVIDE CONTAINMENT OF GASEOUS AND SOLID FISSION PRODUCTS
TRISO	OUTER ISOTROPIC PyC	• PROVIDE MECHANICAL SUPPORT FOR THE SiC LAYER • PROTECT THE SiC FROM DAMAGE DURING HANDLING

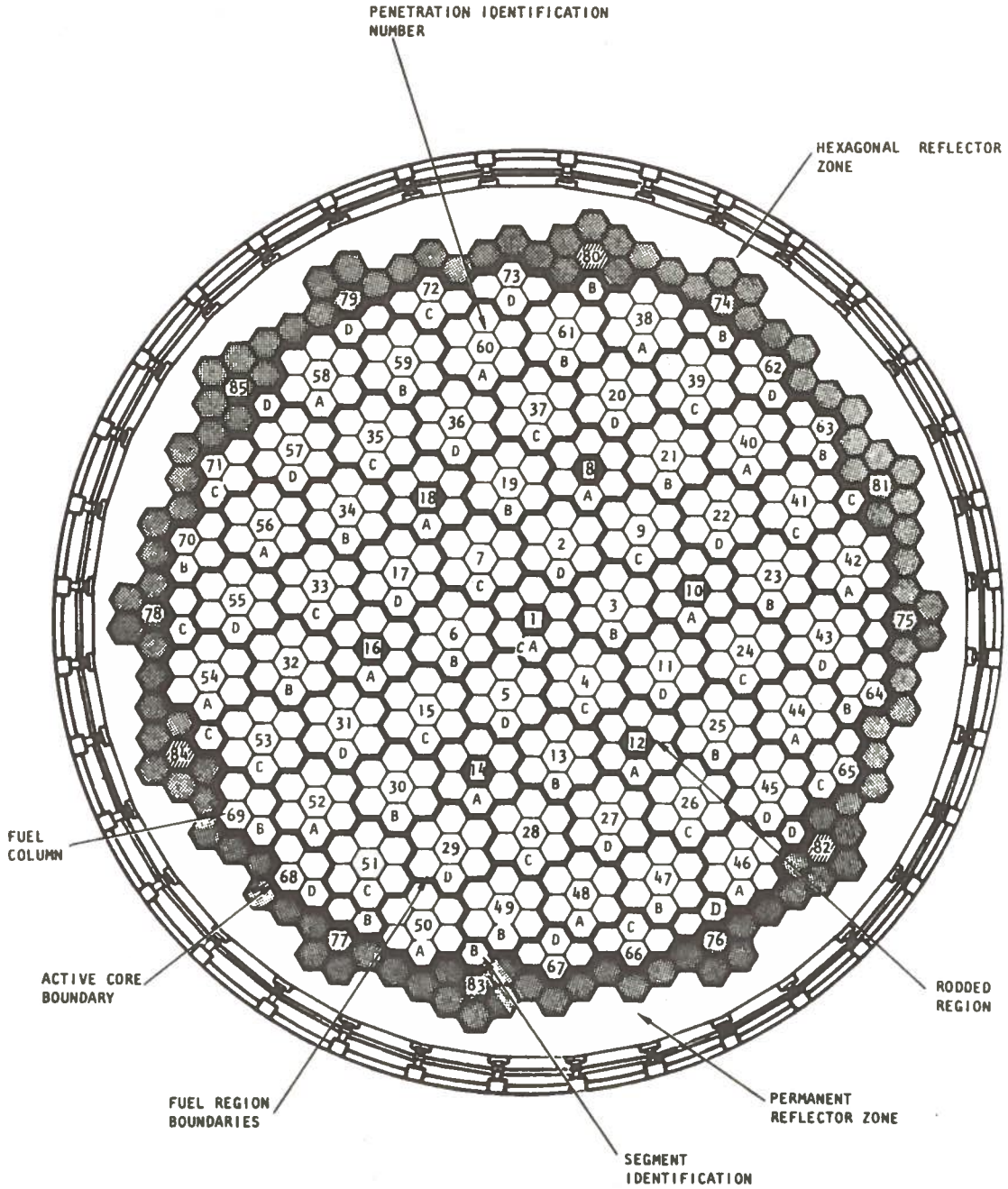

PENETRATION NUMBERS

1-73	CONTROL RODS & ORIFICE VALVES	FUEL COLUMN
74-79,81,83,85	SHIELD PLUGS	REFLECTOR COLUMN
80,82,84	NUCLEAR INSTRUMENTATION	REFLECTOR COLUMN

Fig. 1.4. Core configuration, region and segment identification, for the 1160-MW(e) HTGR[3]

refueling region and is located on a hexagonal refueling penetration which contains a control rod drive assembly. Two parallel channels within the center column are provided for insertion of a pair of control rods. A third channel, within the same column, is built for the insertion of reserve shutdown absorber material. The pressure vessel has a cylindrical shape. One fuel segment is replaced each year. These segments are designated by capital letters A, B, C, and D.

The reflector, which is composed of two components, is made of graphite. One part of the reflector, replaced every eight years, is immediately adjacent to the core. The rest of the reflector is used for the life time of the reactor. An elevation view of the core, reflector, and support structure is shown in Figure 1.5.

The Effects of Temperatures Above 1600°C On Irradiated Fuel Behavior

Irradiated fuel particle behavior as a function of temperature and burnup has been studied in numerous out-of-pile annealing experiments[6]. In these experiments, fuel failure percentages were determined by heating the irradiated fuel particles to a given temperature for a maximum of 100 hours. Temperature-induced-fuel particle failure monitored by measuring release of gaseous fission products was not observed at temperatures less than 1600°C to 100% at 2100°C. Analyzing the data obtained in these experiments, it was assumed that failure varies linearly from pressure vessel value (i.e., fuel failure percentage at normal operating conditions), which is less than 1%, at 1600°C to 100% at 2000°C. It is assumed that for fuel

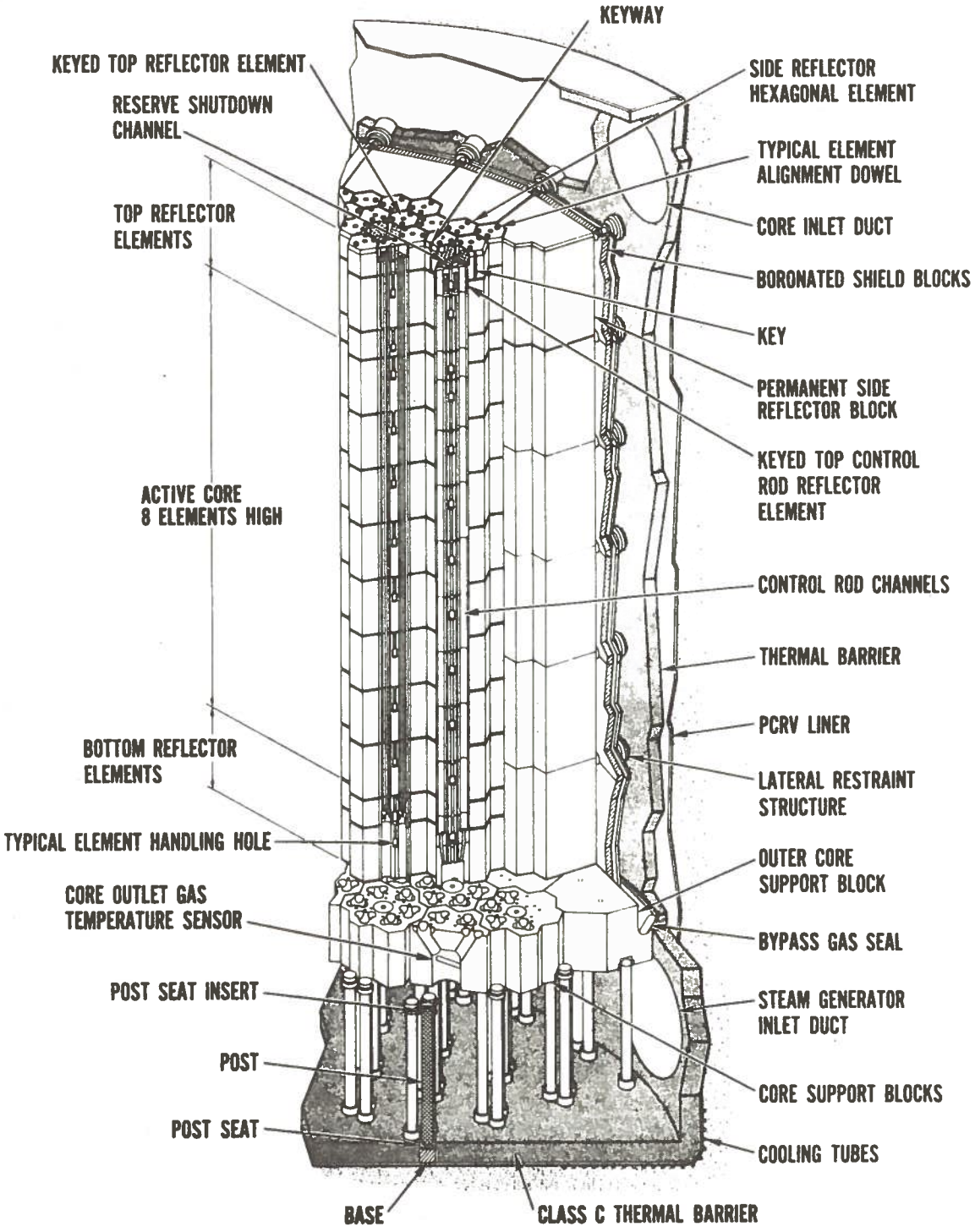

Figure 1.5. Reactor core arrangement[3]

particles with less than 20% burnup failure increases linearly from the pressure vessel value at 1800°C to 100% at 2000°C. This is due to the observation that fuel particles with 20% burnup did not fail until temperatures exceeded 1800°C and to the fact that unirradiated fuel can be heated above 1800°C without failing. For fuel particles irradiated to a peak burnup (78%), it is assumed that failure increases linearly at 1600°C to 100% at 2000°C. The envelop of failure values to be assumed for fuel with various burnups at temperatures exceeding 1600°C is shown in Figure 1.6. Failure predictions for intermediate burnups are made by estimating the critical temperature, T_c, and by assuming that failure increases from the pressure vessel value at T_c to 100% at 2000°C. The critical temperature, which is defined as the temperature at which fuel failure exceeds the pressure vessel value, is assumed to vary linearly from 1600°C at 78% to 1800°C at 20% burnup. The critical temperature is therefore given by

$$T_c = - 3.45(BU) + 1869; \tag{1.1}$$

BU is the fuel burnup and is defined as the percentage of initial metal atoms which have fissioned. The number of initial metal atoms includes both fissile and fertile atoms.

The general equation for the lines given in Figure 1.6 can be derived by taking two known points on the line, namely, $F(T) = 0$, $T = T_c$ and $F(T) = 100\%$, $T = 2000°C$. For temperatures between 1600 and 2000°C this equation is given by

$$F(T) = \frac{100}{2000 - T_c} (T - T_c). \tag{1.2}$$

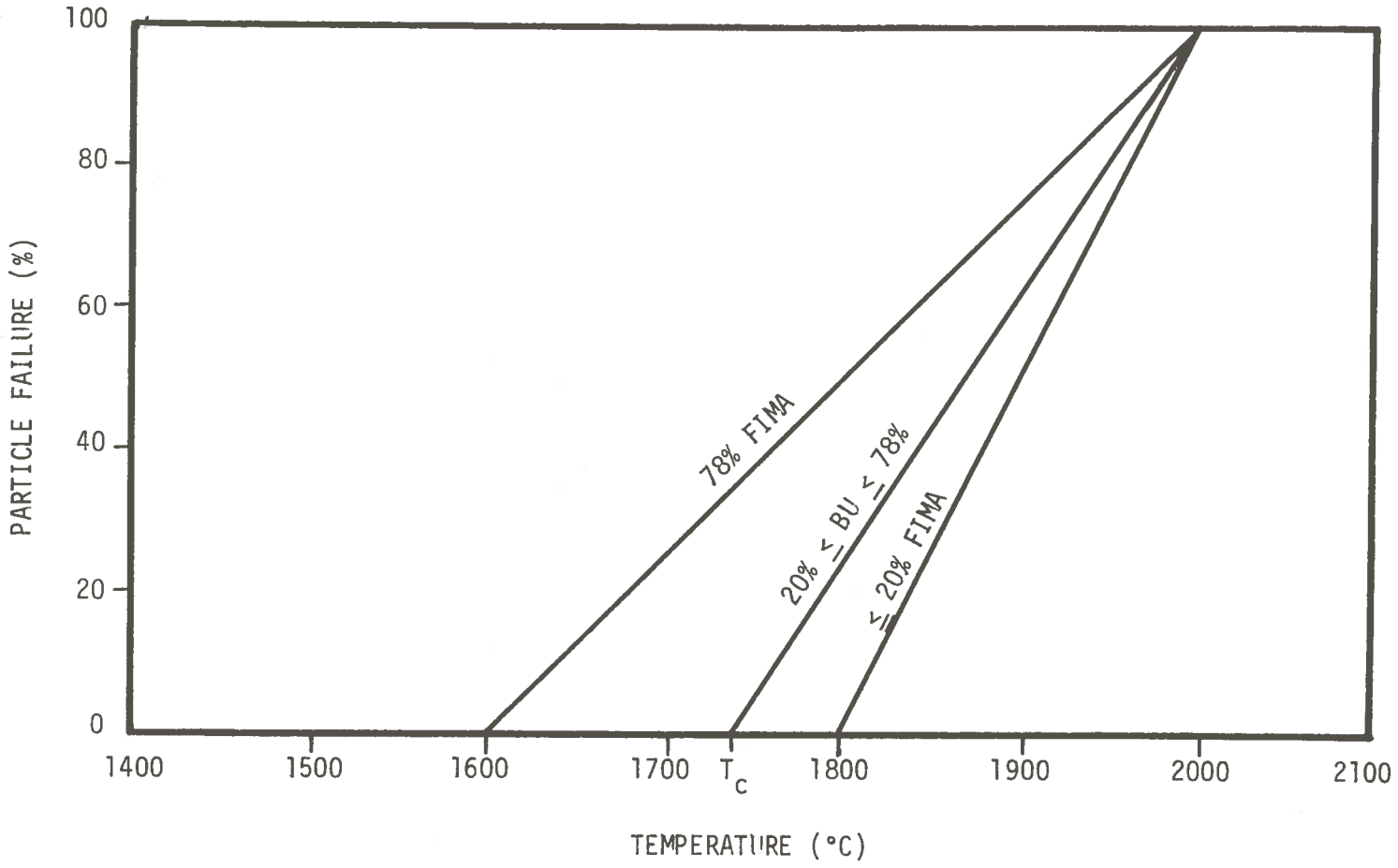

Figure 1.6. Fuel failure assumed during thermal excursions in an operating HTGR

Substituting for T_c in Equation (1.2) yields

$$F(T) = \frac{100}{131 + 3.45\ BU}\ (T - 1869 + 3.45\ BU), \qquad (1.3)$$

in which

F(T) = fuel failure percentage

T = fuel temperature in °C

BU = fuel burnup.

This equation represents fuel failure percentage as a function of temperature for burnups between 20% and 78%. Fuel particles with burnups of less than 20% are conservatively assumed to fail at the same rate as the ones with 20% burnup.

These data provide a method for treating fuel failure during a rapid thermal excursion for temperatures in the range of 1600 to 2000°C. When estimating fuel performance it will be assumed that Equation (1.3) can be used to determine the fraction of fuel failure occurring instantaneously during any given excursion. This equation will give very conservative results because the test data upon which it is based includes the effects of holding at a given temperature for a maximum of 100 hours.

Statement of the Thesis Problem

The basic goal of this thesis is to estimate the fuel failure as a function of time following a design basis depressurization accident, DBDA, for different fuel burnups (or reactor operating times). Since the fuel failure following a DBDA in the HTGR depends primarily upon the post-accident temperature response of the core,

a general equation for the reactor core temperature as a function of time after shutdown will first be developed by considering the heat released in the core because of the decay of fission products. The coupling of this equation with that given in the previous section, which describes the fuel failure as a function of its temperature, will make it possible to predict some lower limit on the time required for various percentages of fuel particle failure following a DBDA. Although a number of different models, discussed in the next chapter, with varying degrees of accuracy can be used to assess the temperature response of the core, this thesis will focus on insights to the problem of fuel failure that can be gained by use of a homogeneous adiabatic heat transfer model. This model assumes a homogeneous distribution of fission products and no heat transfer from the reactor core.

Chapter II

THEORETICAL CONSIDERATIONS

Introduction

The design basis depressurization accident followed by auxiliary circulators failure can cause an increase in the core temperature which could in turn lead to the release of fission products from the temperature-induced-failed fuel particles. There are a number of different models with varying degrees of accuracy that can be used to determine the temperature response of the core following a DBDA in a high temperature gas cooled reactor. Some of these possible models will be discussed briefly.

1. Assume instantaneous release of fission products from fuel particles in the core at the time of accident. This assumption is overly conservative because at this time the average fuel temperature is way below the critical temperature which is the temperature at which fuel failure occurs.
2. Assume homogeneous adiabatic heat transfer conditions. This is equivalent to failure of all circulators and no convection cooling in the reactor core.
3. Assume auxiliary circulators fail and there is only convection cooling in the core.

4. Assume that auxiliary circulators are operating. In this case there will be no fission product release except the primary coolant and "lifted off" activities. These activities are due to the presence of fission products released by the failed fuels operating under normal conditions. "Lift off" refers to primary coolant plateout activities lifted off the primary coolant loop surfaces by the strong flow of the coolant escaping the core following a DBDA.

This thesis uses a homogeneous adiabatic heat transfer model, Assumption 2, to develop a general equation describing the post-accident temperature response of the reactor core as a function of time following a DBDA. This model assumes a homogeneous distribution of fission products.

Growth and Decay of Fission Products in A Reactor Core

To determine the amount of individual fission products in a nuclear reactor, it is necessary to take into account the production of any nuclide by fission as well as by radioactive decay of the parent nuclide, and to allow for removal of any nuclide by neutron absorption as well as by radioactive decay.

Consider a reactor containing N_f fissionable atoms and operating at a constant power level so that the fission rate is constant. The different species of radioactive atoms in a decay chain

can be represented by

$$A_1 \xrightarrow{\lambda_1} A_2 \xrightarrow{\lambda_2} A_3 \xrightarrow{\lambda_3} \cdots \xrightarrow{\lambda_{i-1}} A_i \xrightarrow{\lambda_i} \cdots \quad .$$

For the case of continuous and uniform irradiation, the production and removal processes can be represented as shown in Table 1.4.

Table 1.4

Formation and Removal of Fission Products in the Reactor Core

Formation		Removal	
Fission	Decay	Decay	Burnout
$N_f \sigma_f \phi y_1$	--	$A_1 \lambda_1$	$A_1 \sigma_1 \phi$
$N_f \sigma_f \phi y_2$	$A_1 \lambda_1$	$A_2 \lambda_2$	$A_2 \sigma_2 \phi$
$N_f \sigma_f \phi y_3$	$A_2 \lambda_2$	$A_3 \lambda_3$	$A_3 \sigma_3 \phi$
.	.	.	.
.	.	.	.
.	.	.	.
$N_f \sigma_f \phi y_i$	$A_{i-1} \lambda_{i-1}$	$A_i \lambda_i$	$A_i \sigma_i \phi$

Consulting Table 1.4, the system of differential equations governing the abundance of the nuclides is

$$\frac{dA_1}{d\tau} = N_f \sigma_f \phi y_1 - A_1 \lambda_1 - A_1 \sigma_1 \phi \,, \tag{2.1}$$

$$\frac{dA_2}{d\tau} = N_f \sigma_f \phi y_2 + A_1 \lambda_1 - A_2 \lambda_2 - A_2 \sigma_2 \phi \,,$$

$$\frac{dA_3}{d\tau} = N_f \sigma_f \phi y_3 + A_2 \lambda_2 - A_3 \lambda_3 - A_3 \sigma_3 \phi \,,$$

$$\frac{dA_i}{d\tau} = N_f \sigma_f \phi y_i + A_{i-1} \lambda_{i-1} - A_i \sigma_i \phi \,.$$

Letting

$$\lambda_i + \sigma_i \phi = U_i; \text{ and} \tag{2.2}$$

$$N_f \sigma_f \phi = F, \tag{2.3}$$

then, by substitution,

$$\frac{dA_1}{d\tau} = y_1 F - U_1 A_1 \,, \tag{2.4}$$

$$\frac{dA_2}{d\tau} = \lambda_1 A_1 + y_2 F - U_2 A_2 \,,$$

$$\frac{dA_3}{d\tau} = \lambda_2 A_2 + y_3 F - U_3 A_3 ,$$

.

.

.

$$\frac{dA_i}{d\tau} = \lambda_{i-1} A_{i-1} + y_i F - U_i A_i .$$

In these equations:

σ_f = fission cross section

N_f = number of fissionable atoms

ϕ = average neutron flux

y_i = direct fission yield of the $i^{\underline{th}}$ fission product

λ_i = decay constant of the $i^{\underline{th}}$ isotope

U_i = depletion rate of the $i^{\underline{th}}$ isotope

A_i = number of atoms of the $i^{\underline{th}}$ nuclide

F = fission interaction rate

τ = reactor operating time

Note that since λ_i, σ_i, ϕ, N_f, and σ_f are constant, U_i and F, the interaction rate, are also constant.

Assuming a clean reactor core, the number of atoms of any fission product or fission product daughter present at time $\tau = 0$ (reactor startup time) is zero. The abundance of these nuclides as a function

of reactor operating time, τ, can be obtained by solving the system of differential equations.

The solution is given by

$$A_i(\tau) = e^{-U_i \tau} \int_0^{\tau} [\lambda_{i-1} A_{i-1}(\xi) + y_i F] e^{U_i \xi} d\xi \quad . \tag{2.5}$$

For convinience define the following relations[7]:

$$E(U_i) = e^{-U_i \tau} \quad ; \tag{2.6}$$

$$E(U_i, U_j) = \frac{E(U_i) - E(U_j)}{U_j - U_i} \quad ; \text{ and} \tag{2.7}$$

$$E(U_i, U_j, \ldots, U_k, U_\ell) = \frac{E(U_i, U_j, \ldots, U_k) - E(U_j, \ldots, U_k, U_\ell)}{U_\ell - U_i} . \tag{2.8}$$

The E terms have the important property of being symmetric function of their arguments; that is

$$E(U_i, U_j, \ldots, U_k, U_\ell) = E(U_i, U_\ell, U_j, \ldots, U_k)$$

$$= E(U_\ell, U_i, U_k, U_j, \ldots) = \ldots . \tag{2.9}$$

In particular,

$$E(U_1, U_2) = E(U_2, U_1) \quad ; \text{ and} \tag{2.10}$$

$$E(0, U_1, U_2) = E(0, U_2, U_1) = \ldots . \tag{2.11}$$

Using these relations, the solution will take the following form:

$$i = 1: \quad A_1 = y_1 \, F \, E(0, U_1) \, , \tag{2.12}$$

$$i = 2: \quad A_2 = y_1 \, F \, \lambda_1 \, E(0, \, U_2) + y_2 \, F \, E(0, U_2),$$

$$i = 3: \quad A_3 = y_1 \, F \, \lambda_1 \, \lambda_2 \, E(0, U_1, U_2, U_3) + y_2 \, F \, \lambda_2 \, E(0, U_2, U_3),$$

$$+ y_3 \, F \, E(0, U_3)$$

$$i = 4: \quad A_4 = y_1 \, F \, \lambda_1 \, \lambda_2 \, \lambda_3 \, E(0, U_1, U_2, U_3, U_4) + y_2 \, F \, \lambda_2 \, \lambda_3$$

$$E(0, U_2, U_3, U_4) + y_3 \, F \, \lambda_3 \, E(0, U_3, U_4)$$

$$+ y_4 \, F \, E(0, U_4) \, ,$$

.

.

.

or, in general,

$$A_i(\tau) = F \sum_{\alpha=1}^{i} y_\alpha \frac{\lambda_\alpha \, \lambda_{\alpha+1} \cdots \lambda_i}{\lambda_i} \, E(0, U_\alpha, U_{\alpha+1}, \ldots, U_i) \, ,$$

$$i = 1, 2, 3, \ldots . \tag{2.13}$$

Equation (2.13) represents the number of atoms of the $i^{\underline{th}}$ nuclide as a function of operating time in a nuclear reactor core.

Decay of Fission Products After Reactor Shutdown

Equation (2.13) gives the number of the $i^{\underline{th}}$ fission product after the reactor has been run at stated conditions for a

specified time. If the reactor is then shutdown, the different species of radioactive atoms in a decay chain can be represented by

$$B_1 \xrightarrow{\lambda_1} B_2 \xrightarrow{\lambda_2} B_3 \xrightarrow{\lambda_3} \cdots \xrightarrow{\lambda_{i-1}} B_i \xrightarrow{\lambda_i} \cdots .$$

Then the system of differential equation governing the abundance of these nuclides is

$$\frac{dB_1}{dt} = \lambda_1 B_1 , \tag{2.14}$$

$$\frac{dB_2}{dt} = \lambda_2 B_2 + \lambda_1 B_1 ,$$

$$\frac{dB_3}{dt} = \lambda_3 B_3 + \lambda_2 B_2 ,$$

$$\vdots$$

$$\frac{dB_i}{dt} = \lambda_i B_i + \lambda_{i-1} B_{i-1} .$$

If the number of atoms at the time of reactor shutdown, $t = 0$, are $B_{10}, B_{20}, B_{30}, \ldots, B_{io}$, then the abundance of these nuclides as a function of time after reactor shutdown, t, can be obtained by solving the above system of differential equation. This solution is given by

$$B_i(t) = e^{-\lambda_i t} \int_o^t \lambda_{i-1} B_{i-1}(\xi) e^{-\lambda_i \xi} d\xi + B_{io}(t) e^{-\lambda_i t} . \tag{2.15}$$

Using the relation for E terms given by Equation (2.9), the solution of these differential equations can be expressed in the following form:

$$i = 1: \quad B_1(t) = B_{10}\, E(\lambda_1) \,, \tag{2.16}$$

$$i = 2: \quad B_2(t) = \lambda_1\, B_{10}\, E(\lambda_1, \lambda_2) + B_{20}\, E(\lambda_2) \,,$$

$$i = 3: \quad B_3(t) = \lambda_1\, \lambda_2\, B_{10}\, E(\lambda_1, \lambda_2, \lambda_3) + \lambda_2\, B_{20}\, E(\lambda_2, \lambda_3) \,,$$

.

.

.

or, in general,

$$B_i(t) = \sum_{\beta=1}^{i} \frac{\lambda_\beta\, \lambda_{\beta+1} \cdots \lambda_i}{\lambda_i}\, B_{\beta 0}\, E(\lambda_\beta, \lambda_{\beta+1}, \ldots, \lambda_i) \,, \tag{2.17}$$

$$i = 1, 2, 3, \ldots.$$

In this equation:

t = time after reactor shutdown

λ_i = decay constant of the i^{th} nuclide

$$B_{\beta 0} = A_\beta(\tau = T)$$

$$= F \sum_{\alpha=1}^{\beta} y_\alpha \frac{\lambda_\alpha\, \lambda_{\alpha+1} \cdots \lambda_\beta}{\lambda_\beta}\, E(0, U_\alpha, U_{\alpha+1}, \ldots, U_\beta) \Big|_{\tau = T}$$

T = reactor operating time prior to shutdown

Equation (2.17) represents a general expression for the number of atoms of the $i^{\underline{th}}$ species in the decay chain as a function of time after reactor shutdown in a reactor core.

Heat Released in A Reactor Core Because of The Decay of Fission Products

After a reactor has been shutdown, heat continues to be released in the fuel from the decay of fission products. In this section we will develop a general expression for the total heat released in the reactor core as a function of time after shutdown.

The activity (or disintegration rate) of each nuclide at any time is obtained by multiplying the number of atoms of that nuclide present at any time t by its decay constant:

$$\text{activity of the } i^{\underline{th}} \text{ nuclide} = \lambda_i B_i(t) , \tag{2.18}$$

in which $B_i(t)$ is given by Equation (2.17).

The rate of energy released is then given by

$$\frac{dQ_i(t)}{dt} = R_i \lambda_i B_i(t)$$

$$= R_i \lambda_i \sum_{\beta=1}^{i} \frac{\lambda_\beta \lambda_{\beta+1} \cdots \lambda_i}{\lambda_i} B_{\beta_0} E(\lambda_\beta, \lambda_{\beta+1}, \ldots, \lambda_i) . \tag{2.19}$$

In this equation:

R_i = disintegration energy absorbed by the fuel in MeV

$\simeq 0.34(q_i - \bar{E}_{\gamma i}) + \bar{E}_{\gamma i} = 0.34\ q_i + .66\ \bar{E}_{\gamma i}$

q_i = average disintegration energy in MeV for the $i^{\underline{th}}$ nuclide.

$\bar{E}_{\gamma i}$ = average gamma energy per disintegration for the $i^{\underline{th}}$ nuclide.

Integration of Equation (2.19) will give the energy or heat absorbed by the fuel as a function of time t:

$$Q_i(t) = \int_o^t R_i \lambda_i \sum_{\beta=1}^{i} \frac{\lambda_\beta \lambda_{\beta+1} \cdots \lambda_i}{\lambda_i} B_{\beta_0} E(\lambda_\beta, \lambda_{\beta+1}, \ldots, \lambda_i) \, d\xi$$

$$= R_i \lambda_i \sum_{\beta=1}^{i} \frac{\lambda_\beta \lambda_{\beta+1} \cdots \lambda_i}{\lambda_i} B_{\beta_0} \int_o^t E(\lambda_\beta, \lambda_{\beta+1}, \ldots, \lambda_i) \, d\xi \, . \tag{2.20}$$

For convenience, define

$$I_i(t) = \int_o^t E(\lambda_\beta, \lambda_{\beta+1}, \ldots, \lambda_i) \, d\xi \, , \tag{2.21}$$

in which the terms may be expressed as

$$E(\lambda_\beta, \lambda_{\beta+1}, \ldots, \lambda_i)$$

$$= \frac{E(\lambda_\beta)}{(\lambda_{\beta+1} - \lambda_\beta) \cdots (\lambda_{i-1} - \lambda_\beta) (\lambda_i - \lambda_\beta)}$$

$$+ \frac{E(\lambda_{\beta+1})}{(\lambda_\beta - \lambda_{\beta+1}) \cdots (\lambda_{i-1} - \lambda_{\beta+1}) (\lambda_i - \lambda_{\beta+1})}$$

$$+ \cdots + \frac{E(\lambda_{i-1})}{(\lambda_\beta - \lambda_{i-1}) (\lambda_{\beta+1} - \lambda_{i-1}) \cdots (\lambda_i - \lambda_{i-1})}$$

$$+ \frac{E(\lambda_i)}{(\lambda_\beta - \lambda_i) (\lambda_{\beta+1} - \lambda_i) \cdots (\lambda_{i-1} - \lambda_i)} \, . \tag{2.22}$$

Note that the symmetry of the E terms, Equation (2.9), can be demonstrated by expressing the terms in the form given above.

Substituting this form for the E terms in the integral, the $I_i(t)$ term becomes

$$I_i(t) = \int_o^t \Bigg[\frac{E(\lambda_\beta)}{(\lambda_{\beta+1} - \lambda_\beta)\ldots(\lambda_{i-1} - \lambda_\beta)\ (\lambda_i - \lambda_\beta)}$$

$$+ \frac{E(\lambda_{\beta+1})}{(\lambda_\beta - \lambda_{\beta+1})\ldots(\lambda_{i-1} - \lambda_{\beta+1})\ (\lambda_i - \lambda_{\beta+1})}$$

$$+ \ldots + \frac{E(\lambda_{i-1})}{(\lambda_\beta - \lambda_{i-1})\ (\lambda_{\beta+1} - \lambda_{i-1})\ldots(\lambda_i - \lambda_{i-1})}$$

$$+ \frac{E(\lambda_i)}{(\lambda_\beta - \lambda_i)\ (\lambda_{\beta+1} - \lambda_i)\ldots(\lambda_{i-1} - \lambda_i)} \Bigg] d\xi$$

$$= \frac{1 - E(\lambda_\beta)}{\lambda_\beta(\lambda_{\beta+1} - \lambda_\beta)\ldots(\lambda_{i-1} - \lambda_\beta)\ (\lambda_i - \lambda_\beta)}$$

$$+ \frac{1 - E(\lambda_{\beta+1})}{\lambda_{\beta+1}\ (\lambda_\beta - \lambda_{\beta+1})\ldots(\lambda_{i-1} - \lambda_{\beta+1})\ (\lambda_i - \lambda_{\beta+1})}$$

$$+ \ldots + \frac{1 - E(\lambda_{i-1})}{\lambda_{i-1}\ (\lambda_\beta - \lambda_{i-1})\ (\lambda_{\beta+1} - \lambda_{i-1})\ldots(\lambda_i - \lambda_{i-1})}$$

$$+ \frac{1 - E(\lambda_i)}{\lambda_i\ (\lambda_\beta - \lambda_i)\ (\lambda_{\beta+1} - \lambda_i)\ldots(\lambda_{i-1} - \lambda_i)} \quad . \qquad (2.23)$$

Equation (2.23) can be written in the following summation form:

$$I_i(t) = \sum_{\alpha=\beta}^{\alpha=i} \frac{1 - E(\lambda_\alpha)}{\lambda_\alpha} \prod_{\substack{J=\beta \\ J\neq\alpha}}^{J=i} \frac{1}{\lambda_j - \lambda_\alpha} \quad ; \tag{2.24}$$

or

$$I_i(t) = \sum_{\alpha=\beta}^{\alpha=i} E(0, \lambda_\alpha) \prod_{\substack{J=\beta \\ J\neq\alpha}}^{J=i} \frac{1}{\lambda_j - \lambda_\alpha} \quad . \tag{2.25}$$

Equation (2.25) may be substituted into Equation (2.20) to obtain

$$Q_i(t) = R_i \lambda_i \sum_{\beta=1}^{\beta=i} \left[\frac{\lambda_\beta \lambda_{\beta+1} \cdots \lambda_i}{\lambda_i} B_{\beta 0} \sum_{\alpha=\beta}^{\alpha=i} E(0,\lambda_\alpha) \prod_{\substack{J=\beta \\ J\neq\alpha}}^{J=i} \frac{1}{\lambda_j - \lambda_\alpha}\right] . \tag{2.26}$$

Since in each fuel element there may be N radioactive nuclides which are decaying simultaneously, the energy absorbed (or released) can be obtained by adding the contributions of all N nuclides. This can be represented by

$$Q_T(t) = \sum_{K=1}^{N} Q_{iK}(t) \quad ; \tag{2.27}$$

or

$$Q_T(t) = \sum_{K=1}^{N} R_{iK} \lambda_{iK} \sum_{\beta=1}^{\beta=i} \left[\frac{\lambda_{\beta K} \lambda_{(\beta+1)K} \cdots \lambda_{iK}}{\lambda_{iK}} B_{\beta_0 K} \right.$$

$$\left. X \sum_{\alpha=\beta}^{\alpha=i} E(0, \lambda_{\alpha K}) \prod_{\substack{J=\beta \\ J\neq\alpha}}^{J=i} \frac{1}{\lambda_{jK} - \lambda_{\alpha K}}\right] , \tag{2.28}$$

in which

i represents the position of the nuclide in a particular decay chain

K is the identification number of that isotope

$$\prod_{\substack{J=\beta \\ J\neq\alpha}}^{J=i} \frac{1}{\lambda_j - \lambda_\alpha} = \frac{1}{\lambda_\beta - \lambda_\alpha} \cdot \frac{1}{\lambda_{\beta+1} - \lambda_\alpha} \cdots \frac{1}{\lambda_{i-1} - \lambda_\alpha} \cdot \frac{1}{\lambda_i - \lambda_\alpha}$$

and

$$\frac{1}{\lambda_j - \lambda_\alpha} \equiv 1 \text{ for } j = \alpha \ .$$

Note: the summation in Equation (2.28) is over K rather than i, because i simply denotes the position of the isotope in a particular decay chain.

Equation (2.28) represents the general expression for the total heat released (or absorbed), in MeV, because of the decay of fission products in the fuel as a function of time after shutdown.

Reactor Core Temperature as A Function of Time Following A Design Basis Depressurization Accident

Since the fuel failure following a design basis depressurization accident in the HTGR depends primarily upon the post-accident temperature response of the core. We will, at this stage, develop the general equation for the core temperature as a function of time following a DBDA. Although a number of different models with varying degrees of accuracy can be used to obtain the temperature response of the reactor, we will focus on the insights to this problem that can be gained by use of the homogeneous adiabatic heat transfer model previously discussed in this chapter.

The heat released in the fuel following a DBDA will be due to the decay heat only since the reactor is immediately shutdown at the onset of the accident. The relationship between the total heat released in the fuel and the core temperature is given by

$$(3.827 \times 10^{-14} \frac{cal}{MeV})\ Q_T(t) = m\bar{C}p\ \Delta T \qquad (2.29)$$

provided that there is no heat transferred from the core.

In the above equation:

$Q_T(t)$ = total heat released in the fuel in MeV

m = mass of the fuel in grams

$\bar{C}p$ = average specific heat in calories/gram

ΔT = change in core (or fuel) temperature in °C

$= T(t) - T_o$

$T(t)$ = final temperature of the core as a function of time in °C

T_o = average operating temperature of the core in °C.

3.827×10^{-14} = conversion factor from MeV to calories

Note that the fuel and the moderator are assumed to be at the same temperature; that is, the fuel is assumed to be homogeneously distributed in the core.

Equation (2.29) can be solved for T(t). This gives

$$T(t) = \frac{3.827 \times 10^{-14}}{m\bar{C}p}\ Q_T(t) + T_o \qquad (2.30)$$

Inserting Equation (2.29) into Equation (2.28), the temperature is now

$$T(t) = T_o + \frac{3.827 \times 10^{-14}}{m\bar{C}p} \sum_{K=1}^{N} R_{iK} \lambda_{iK} \sum_{\beta=1}^{\beta=i}$$

$$\left[\frac{\lambda_{\beta K} \lambda_{(\beta+1)K} \cdots \lambda_{iK}}{\lambda_{iK}} B_{\beta_0 K} \sum_{\alpha=\beta}^{\alpha=i} E(0, \lambda_{\alpha K})\right.$$

$$\left. \prod_{\substack{J=\beta \\ J\neq\alpha}}^{J=i} \frac{1}{\lambda_{jK} - \lambda_{\alpha K}} \right] . \qquad (2.31)$$

Equation (2.31) describes the post-accident temperature response of the reactor core as a function of time following a DBDA.

Some Special Cases

In the proceeding section an equation, Equation (2.31), was developed for the post-accident temperature of the core as a function of time following the DBDA. In this equation the decay heat due to all of the radioactive nuclides in the decay chain was taken into account. In the following discussion, we will first consider three special cases in which we assume up to one, two, and three radioactive nuclides in the decay chain respectively. Then, for comparison, the core temperature will be approximated by means of two different empirical expressions for the rate of energy released in the core due to decay of fission products given by Way and Wigner[8] and Stehn and Clancy[9], respectively.

First approximation. In this case it is assumed that all radioactive nuclides decay to a stable isotope.

Hence, letting i = 1 in Equation (2.31) gives

$$T(t) = T_o + \frac{3.827 \times 10^{-14}}{m\bar{C}p} \sum_{K=1}^{N} R_{1K} \lambda_{1K} B_{10K} E(0, \lambda_{1K}) . \quad (2.33)$$

Equation (2.33) represents the "first approximation" of the post-accident temperature response of the reactor core as a function of time following a DBDA.

Second approximation. In this case we assume up to two radioactive nuclides in the decay chain. Hence, the temperature response in the core is obtained by setting i = 2 in Equation (2.31); that is,

$$T(t) = T_o + \frac{3.827 \times 10^{-14}}{m\bar{C}p} \sum_{K=1}^{N} R_{2K} \lambda_{2K} \left[\lambda_{1K} B_{10K} \left(\frac{E(0, \lambda_{1K})}{\lambda_{1K} - \lambda_{1K}} + \frac{E(0, \lambda_{2K})}{\lambda_{1K} - \lambda_{2K}}\right) + B_{20K} E(0, \lambda_{2K})\right] . \quad (2.34)$$

Equation (2.34) represents the "second approximation" of the post-accident temperature response of the core as a function of time following a DBDA.

Third approximation. In this case we will assume up to three radioactive nuclides in the decay chain. Thus the temperature as a function of time can be determined by setting i = 3 in Equation (2.31);

that is,

$$T(t) = T_o + \frac{3.827 \times 10^{-14}}{m\bar{C}p} \sum_{K=1}^{N} R_{3K}\,\lambda_{3K}\,[\,\lambda_{1K}\,\lambda_{2K}\,B_{10K}$$

$$\left(\frac{E(0,\lambda_{1K})}{(\lambda_{1K}-\lambda_{1K})(\lambda_{3K}-\lambda_{1K})} + \frac{E(0,\lambda_{2K})}{(\lambda_{1K}-\lambda_{2K})(\lambda_{3K}-\lambda_{2K})}\right.$$

$$\left. + \frac{E(0,\lambda_{3K})}{(\lambda_{1K}-\lambda_{3K})(\lambda_{2K}-\lambda_{3K})}\right)$$

$$+ \lambda_{2K}\,B_{20K}\left(\frac{E(0,\lambda_{2K})}{\lambda_{3K}-\lambda_{2K}} + \frac{E(0,\lambda_{3K})}{\lambda_{2K}-\lambda_{3K}}\right)$$

$$+ B_{30K}\,E(0,\lambda_{3K})\,]\,. \qquad (2.35)$$

Equation (2.35) represents the "third approximation" of the post-accident temperature response of the reactor core as a function of time following a DBDA.

Borst-Wheeler approximation[10]. Way and Wigner[8] gave a theoretical treatment, of the rate of energy released in the reactor core due to the decay of fission products, based on the Weizsacker semi-empirical mass formula[11]. They reduced their results to the empirical relations given below which fit the experimental values obtained by Perkins and King[12] rather well over a large span of decay times.

$$\dot{E}_{\beta}(t) = 1.26\ t^{-1.2} \quad \text{MeV/sec - fission,} \tag{2.36}$$

$$\dot{E}_{\gamma}(t) = 1.4\ t^{-1.2} \quad \text{MeV/sec - fission,} \tag{2.37}$$

in which

$\dot{E}_{\beta}(t)$ = the average energy in MeV emitted per second in the form of beta particles t sec after one fission

$\dot{E}_{\gamma}(t)$ = the average energy in MeV emitted per second in the form of gamma ray photons t sec after one fission.

These equations are valid for $1 \leq t \leq 10^6$ sec.

The total rate of energy released from decaying fission products is therefore given by

$$\dot{E}_{T}(t) = \dot{E}_{\beta}(t) + \dot{E}_{\gamma}(t). \tag{2.38}$$

Or

$$\dot{E}_{T}(t) = 2.66\ t^{-1.2} \quad \text{MeV/sec - fission.} \tag{2.39}$$

For a reactor operating at a constant power level Po watts for T second, the total energy released at time t second after shutdown can be obtained by integrating Equation (2.39) over the entire period of operation. That is,

$$E_{T}(t, T) = C \int_{o}^{T} P_{o}\, \dot{E}(t + \xi)\, d\xi\ . \tag{2.40}$$

Here, C is equal to 3.1×10^{10} fission/watt - sec which is conservatively based on the recoverable energy of 200 MeV/fission.

Hence, by substituting Equation (2.39) in Equation (2.40), we get

$$E_T(t, T) = 3.1 \times 10^{10} P_o \int_o^T 2.66 (t + \xi)^{-1.2} d\xi , \qquad (2.41)$$

or

$$E_T(t + T) = 4.1 \times 10^{11} P_o [t^{-0.2} - (t + T)^{-0.2}] \text{ MeV/sec.} \qquad (2.42)$$

Equation (2.42) is normally known as the Borst-Wheeler function.

Total heat generation, $Q_T(t)$, at any time after reactor shutdown will be determined by integrating the total energy released, Equation (2.42), from reactor shutdown time (t = 0) to an arbitrary time t.

Therefore,

$$Q_T(t) = \int_o^t E_T(\xi, T) d\xi , \qquad (2.43)$$

or

$$Q_T(t) = \int_o^t 4.1 \times 10^{11} P_o [\xi^{-0.2} - (\xi + T)^{0.2}] d\xi$$

or

$$Q_T(t) = 5.12 \times 10^{11} P_o \left[t^{0.8} - (t + T)^{0.8} + T^{0.8}\right] \text{ MeV.} \quad (2.44)$$

Now, assuming a homogeneous adiabatic heat transfer model, the total heat generated, $Q_T(t)$, can be related to the post-accident temperature response of the reactor core, T(t), following a DBDA by

$$(3.827 \times 10^{-14} \frac{\text{cal}}{\text{MeV}})\ Q(t) = m\bar{C}p\ (T(t) - T_o), \quad (2.45)$$

in which the constants 3.827×10^{-14} cal/MeV, m, $\bar{C}p$, and T_o are defined on page 31.

Substituting Equation (2.24) in Equation (2.45) and solving for T(t):

$$T(t) = T_o + \frac{1.96 \times 10^{-2} P_o}{m\bar{C}p} \left[t^{0.8} - (t + T)^{0.8} + T^{0.8}\right] . \quad (2.46)$$

Equation (2.46) represents the Borst-Wheeler approximation of post-accident temperature response of the reactor core as a function of time following a DBDA.

Stehn and Clancy approximation[9]. The rate of energy released in the reactor core because of the decay of fission products has been predicted by other empirical relations in addition to those of Way and Wigner discussed in the proceeding section. Stehn and Clancy developed an empirical equation to fit their experimental data reasonably well from 10 seconds to three hours. This equation is given by

$$\dot{E}_T(t) = 4.1\ t^{-1.2}\ \text{MeV/second - fission}$$

in which

$\dot{E}_T(t)$ = the total energy in MeV emitted per second in the form of beta particles and gamma ray photons t seconds after one fission.

Similarly, using Stehn and Clancy's equation, it can be shown that the post-accident temperature response of the reactor core as a function of time following a DBDA is given by

$$T(t) = T_o + \frac{3 \times 10^{-2}\ P_o}{m\bar{C}p}\ [t^{0.8} - (t + T)^{0.8} + T^{0.8}]\ . \qquad (2.48)$$

Equation (2.48) will be called the Stehn and Clancy approximation of the post-accident temperature response of the core as a function of time following a DBDA.

Chapter III

ANALYSIS AND RESULTS

Introduction

In the last chapter, we developed five different types of approximations for estimating the post-accident temperature response of the reactor core as a function of time following a DBDA. We now focus our attention upon the primary goal of this thesis, which is to provide conservative evaluation of the fuel survival fraction as a function of time following a DBDA in the HTGR.

In this chapter the foregoing formulations will be evaluated and then the one judged to be the most realistic will be approximated by a fourth-order interpolating polynomial to simplify calculations. Then, utilizing this polynomial, together with the equation describing the fuel performance as a function of temperature, it will be possible to obtain the fuel failure percentages in the core as a function of time following a DBDA for a burnup of 20% and burnups prior to refueling after one, two, three, and four years of reactor operation.

This analysis will be done for the 1160 MW(e) HTGR with a plant capacity factor of 0.80, which is General Atomic's reference design reactor. The same analysis could be performed for the 770 MW(e) and the 1540 MW(e) HTGR (See Table 1.1); but this will not be attempted here because the fission product inventories are not readily available and it is expected that the results will vary only slightly from those reported in this thesis for the reference design reactor.

Temperature Response of the 1160 MW(e) HTGR

In this section, we will specifically look at the temperature response of the 1160 MW(e) HTGR as a function of time following a DBDA. Five different kinds of approximations for the core temperature were developed in the proceeding chapter. With the use of the TEMP computer program, the first, second, and third approximation of the post-accident temperature response of the core as a function of time following a DBDA were calculated by making the following assumptions.

1. The operating power of the 1160 MW(e) HTGR is 3000 MW(th) with a plant capacity of 0.80.
2. The reactor core contains 3944 fuel elements.
3. The average fuel loading per fuel element is 9.5 kg of Thorium and 0.44 kg of Uranium.
4. All fuel elements are assumed to weigh 116.2 kg, which is the average fuel element weight.
5. The average weight of graphite in a fuel element is assumed to be 106.2 kg.
6. The specific heat[13] for materials of interest are:
   a. Graphite = 0.172 calories/gram-°C
   b. Thorium = 0.0331 calories/gram-°C
   c. Uranium = 0.0276 calories/gram-°C
7. Reactor equlibrium fuel element activities for an average power element after four years of operation are assumed for this analysis. These activities are given in Appendix A.

8. The initial temperature of the reactor fuel is assumed to be 752°C. This is the average core temperature at full power.
9. All beta and gamma disintegration energy from the radioactive nuclide is absorbed by the fuel. The average gamma and beta energy emitted by each nuclide is obtained from reference (14).

The core design parameters of the 1160 MW(e) HTGR given above are tabulated in Appendix B in detail[15]. In this analysis $Q_T(t)$, and hence T(t) in Equation (2.33), (2.34), and (2.35), was computed from the design fission product inventories for the 1160 MW(e) HTGR; the output data of interest are tabulated in Appendix A. A comparison of the first, second, and third approximation of the post-accident temperature response of the 1160 MW(e) HTGR core as a function of time is shown in Figure 3.1.

Utilizing the Borst-Wheeler approximation, Equation (2.46), the temperature response of the 1160 MW(e) HTGR core as a function time following a DBDA can be determined by making the same assumptions as previously mentioned in this section. This is done by first calculating the following parameters in Equation (2.46):

$$P_o = \text{(operating power) x (capacity factor)}$$

$$= 3000 \times 0.80 = 2400 \text{ MW(th)},$$

$$T_o = 752°C,$$

$$m\bar{C}p = m_U C_{PU} + m_{Th} C_{PTh} + m_g C_{Pg},$$

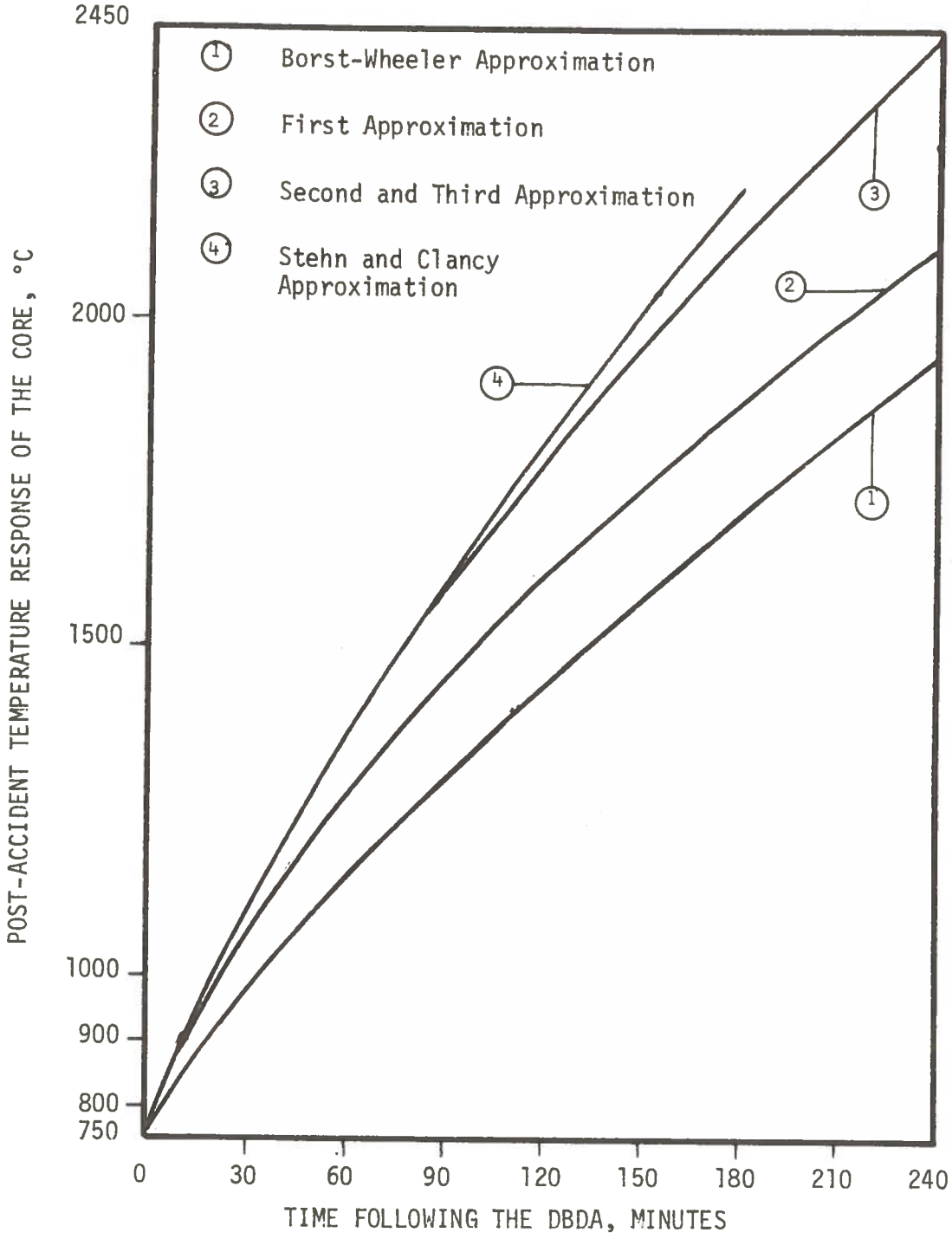

Figure 3.1. Post-accident temperature response of the core as a function of time following the DBDA in the 1160 MW(e) HTGR.

in which

m_U and C_{PU} = the mass and specific heat of Uranium in the core respectively,

m_{Th} and C_{PTh} = the mass and specific heat of Thorium in the core respectively,

and

m_g and C_{Pg} = the mass and specific heat of graphite in the core respectively.

Therefore

$$m\bar{C}p = 7.33 \times 10^7 \text{ calories.}$$

Using these values for P_o and $m\bar{C}p$, Equation (2.46) becomes

$$T(t) = 752 + 0.64\,[t^{0.8} - (t + T) + T^{0.8}]\,,$$

$$\text{for } 1 \leq t \leq 10^6 \text{ seconds.} \qquad (3.1)$$

Similarly, the Stehn and Clancy approximation, Equation (2.48), for the temperature response of the 1160 MW(e) HTGR core can be reduced to

$$T(t) = 752 + 0.98\,[t^{0.8} - (t + T)^{0.8} + T^{0.8}]$$

$$\text{for } 10 \leq t \leq 1.08 \times 10^4 \text{ seconds.} \qquad (3.2)$$

The Borst-Wheeler and Stehn and Clancy approximations are also included in Figure 3.1 for comparison. The data used to plot Equations (3.1) and (3.2) are tabulated below.

Table 3.1

Borst-Wheeler and Stehn and Clancys Approximation of the Post-accident Temperature Response of the Core as a Function Time Following a DBDA in the 1160 MW(e) HTGR

t, Min.	Borst-Wheeler approx. of T in °C	Stehn and Clancy approx. of T in °C
0	752	--
30	987	1110
60	1157	1372
90	1306	1599
120	1443	1811
150	1573	2010
180	1698	2200
210	1818	--
240	1933	--
270	2045	--
300	2154	--

Figure 3.1 is a comparison of the Borst-Wheeler and Stehn and Clancy results for the post-accident temperature response of the 1160 MW(e) HTGR with the present work and reveals that the values obtained by the second and third approximations are in good agreement with those determined by computing T(t) by use of the Stehn and Clancy approximation over the first 180 minutes following the DBDA. Figure 3.1 also indicates that the values given by the second

approximation are larger than those obtained by use of the first approximation. This is what we expected because we assumed more radioactive nuclides in the decay chain in the second approximation than in the case of the first approximation.

Since the third approximation showed no improvement over the second approximation of the core temperature, we will choose the latter approximation for fuel failure analysis as a function of time following a DBDA in the 1160 MW(e) HTGR for our polynomial approximation.

Fourth-Order Interpolating Polynomial

Earlier in Chapter I, we discussed the HTGR irradiated fuel particle behavior as a function of temperature and burnup. It was shown that Equation (1.3) provides a method for treating fuel failure during a thermal excursion for temperatures in the range of 1600 to 2000°C. In order to be able to relate fuel failure percentages to time following the DBDA, we will first find an equation representing the second approximation curve for temperatures up to 2000°C shown in Figure 3.1. The combination of this equation with Equation (1.3) will give the function of interest.

A common method of approximating functions is by use of polynomials. In this section, we therefore find an interpolating polynomial of fourth-order to approximate the temperature response of the core as a function of time following a DBDA in the 1160 MW(e) HTGR for temperatures up to 2000°C using the second approximation data given in Appendix A.

The general method of constructing a polynomial consists of passing an $n^{\underline{th}}$ order polynomial P(t) through n + 1 points. These points are given in a tabular form,

t	T(t)
t_1	$T(t_1)$
t_2	$T(t_2)$
.	
.	
.	
t_n	$T(t_n)$

where the values in the table are assumed to be ordered, that is $t_{i+1} \geq t_i$.

The second approximation curve T(t) in Figure 3.1 can be represented by an $n^{\underline{th}}$ - order polynomial, $P_n(t)$

$$P_n(t) = a_1 t^n + a_2 t^{n-1} + \ldots + a_n t + a_{n+1} \qquad (3.3)$$

by the following procedure:

1. Choose the order of polynomial. In this case we will take n = 4 (i.e., a fourth-order polynomial).
2. Compute n + 1 values of T(t) by choosing n + 1 arbitrary values of t (i.e., t_1, t_2,... t_5 for our case).

3. Rewrite the polynomial $P(t) = a_0 + t^4 + a_2 t^3 + a_3 t^2 + a_4 t + a_5$ in the form

$$P_4(t) = A_1 + A_2 (t - t_1) + A_3 (t - t_1)(t - t_2) + A_4 (t - t_1)(t - t_2)(t - t_3) + A_5 (t - t_1)(t - t_2)(t - t_3)(t - t_4).$$

4. Expand the above polynomial and solve for the a_i's in terms of the A_i's and the selected values of t (i.e., $t_1,\ldots,t_4$). Doing this, we get

$$a_1 = A_5 \tag{3.4}$$

$$a_2 = A_4 - (t_1 + t_2 + t_3 + t_4) A_5 \tag{3.5}$$

$$a_3 = A_3 - (t_1 + t_2 + t_3) A_4 + (t_1 t_2 + t_1 t_3 + t_1 t_4 + t_2 t_3 + t_2 t_4 + t_3 t_4) A_5 \tag{3.6}$$

$$a_4 = A_2 - (t_1 + t_2) A_3 + (t_1 t_2 + t_1 t_3 + t_2 t_3) A_4 - (t_1 t_2 t_3 + t_1 t_2 t_4 + t_1 t_3 t_4 + t_2 t_3 t_4) A_5 \tag{3.7}$$

$$a_5 = A_1 - t_1 A_2 + t_1 t_2 A_3 - t_1 t_2 t_3 A_4 + t_1 t_2 t_3 t_4 A_5 . \tag{3.8}$$

5. In order to solve for A_i's we set $P_4(t_i) = T(t_i)$ to get

$$A_1 = T(t_1) \tag{3.9}$$

$$A_2 = [T(t_2) - A_1]/ (t_2 - t_1) \tag{3.10}$$

$$A_3 = [T(t_3) - A_1 - A_2 (t_3 - t_1)] / (t_3 - t_1) (t_3 - t_2) \quad (3.11)$$

$$A_4 = [T(t_4) - A_1 - A_2 (t_4 - t_1) - A_3 (t_4 - t_1) (t_4 - t_2)]/(t_4 - t_1) (t_4 - t_2) (t_4 - t_3) \quad (3.12)$$

$$A_5 = [T(t_5) - A_1 - A_2 (t_5 - t_1) - A_3 (t_5 - t_1) (t_5 - t_2) - A_4 (t_5 - t_1) (t_5 - t_2) (t_5 - t_3)]/(t_5 - t_1) (t_5 - t_2) (t_5 - t_3) (t_5 - t_4). \quad (3.13)$$

To find the fourth-order interpolating polynomial we will choose five arbitrary data points from Appendix A; that is,

i	1	2	3	4	5
t_i, min.	90	105	120	150	165
$T(t_i)$, °C	1581	1681	1777	1955	2040

Applying the method described above, the polynomial of interest is now given by

$$P_4(t) = 1.3160 \times 10^{-6} t^4 - 6.3658 \times 10^{-4} t^3 + 0.10428 t^2 - 0.38596 t + 1148.8, \quad (3.14)$$

in which $P_4(t) \approx T(t)$ and t are expressed in °C and minutes respectively.

Equation (3.14) is valid for $1581 \leq T \leq 2040°C$ or $90 \leq t \leq 165$ min.

A comparison of Equation (3.14) and the second approximation is shown in Table 3.2 and Figure 3.2. In Figure 3.2 the solid curve represents the second approximation and the solid dots are arbitrary points obtained from Equation (3.14). The solid dots representing the fourth-order polynomial in Figure 3.2 are taken from Table 3.2 constructed by use of Equation (3.14). The agreement between the fourth-order polynomial and second approximation is seen to be very good from Figure 3.2 and Table 3.2. Therefore, from now on, Equation (3.3) is assumed to represent the second approximation of the post-accident temperature response of the core as a function of time following a DBDA in the 1160 MW(e) HTGR.

Linear Approximation

As may be seen from Figure 3.1, at temperatures between 1600 and 2000°C the second approximation may be estimated quite accurately by a straight line instead of by the fourth-order polynomial. A least squares fit of the "second approximation" in that interval gives rise to the following equation for the post-accident temperature response of the core as a function of time following a DBDA in the 1160 MW(e) HTGR.

$$T(t) = 6.098\ t + 1038 \text{ for } 90 \leq t \leq 165 \text{ min.} \qquad (3.15)$$

In this equation T(t) and t are expressed in °C and minutes, respectively.

Table 3.2

A Comparison of the Second Approximation Results for the Post-accident Temperature Response of the Core, T(t), in the 1160 MW(e) HTGR to the Fourth-order Polynomial Results, $P_4(t)$.

t, min.	90	95	100	105	110	115	120	125	130	135	140	145	150	155	160	165
$P_4(t)$, °C	1581	1615	1648	1681	1713	1745	1777	1809	1838	1868	1897	1927	1955	1983	2012	2040
T(t), °C	1581	1615	1648	1681	1715	1747	1777	1809	1840	1868	1898	1926	1955	1983	2012	2040

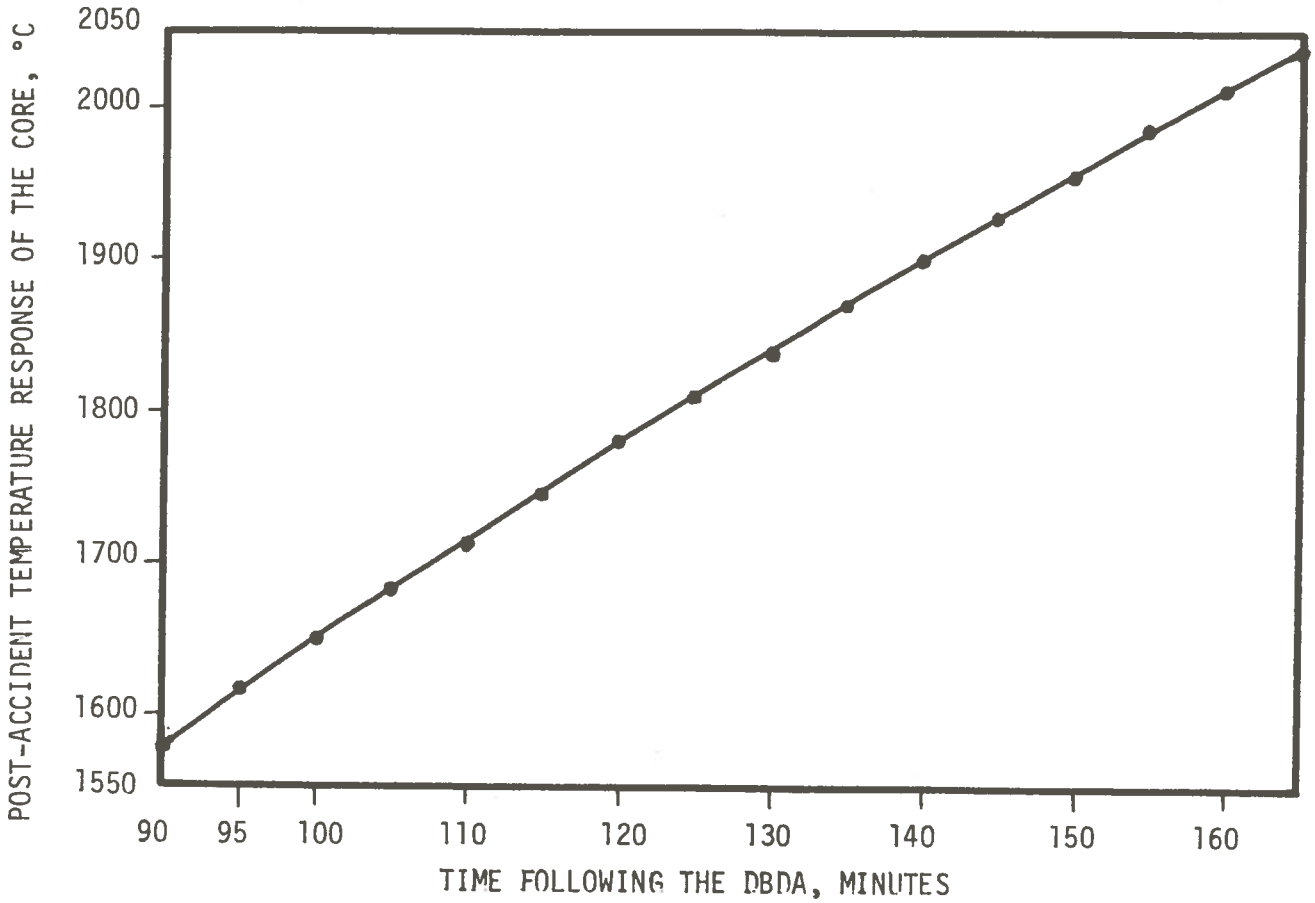

Figure 3.2. A comparison of the second approximation results for the post-accident temperature response of the core in the 1160 MW(e) HTGR to the fourth-order polynomial results. The solid curve represents the second approximation and the solid dots represents the fourth-order polynomial results.

Calculation of Reactor Burnups for Different Reactor Operating Times[10]

In this section, we will first develop an equation for calculating fuel burnup as a function of reactor operating time. Then, using this equation, fuel burnups in the 1160 MW(e) HTGR, for 1, 2, 3, and 4 years of reactor operation will be determined.

The rate of depletion of a fissile isotope is given by[12]

$$\frac{dU(r, \tau)}{d\tau} = - U(r, \tau)\ \bar{\sigma}_a\ \phi_t\ (r, \tau)\ C. \tag{3.16}$$

For a reactor operating at a constant thermal flux, the solution of this equation is

$$U(\tau) = U_o \exp\ (- \bar{\sigma}_a\ \phi_t\ C\ \tau), \tag{3.17}$$

in which:

$U(r,\tau)$ = atom density of the fissile isotope at point r and time τ.

$\bar{\sigma}_a$ = temperature corrected thermal-neutron absorption cross section of the fissile isotope

τ = reactor operating time

ϕ_t = thermal flux in the reactor

c = plant capacity factor

U_o = initial atom density of the fissile isotope.

The number of atoms consumed per unit volume, $U_c(\tau)$, is therefore given by

$$U_c(t) = U_o[1 - \exp(\bar{\sigma}_a \phi_t C \tau)]. \tag{3.18}$$

Using Equation (3.18), we can find the burnup, BU, in time t as follows:

$$BU = (100) \frac{\bar{\sigma}_f}{\bar{\sigma}_a} \frac{U_o[1 - \exp(\bar{\sigma}_a \phi_t C \tau)]}{U_o}, \tag{3.19}$$

in which:

BU = percent fission per initial U-235 atoms,

$\bar{\sigma}_f$ = temperature corrected fission cross section of the isotope (i.e., cross section at temperature T).

But:

$$\bar{\sigma}_f = g_f(T) \frac{\sigma_f(T_o)}{1.128} (T_o/T)^{1/2}, \tag{3.20}$$

and

$$\bar{\sigma}_a = g_a(T) \frac{\sigma_a(T_o)}{1.128} (T_o/T)^{1/2}, \tag{3.21}$$

in which

$g_a(T)$, $g_f(T)$ are respectively the non-$1/\nu$ absorption factor and the fission factor at fuel temperature T,

T_o is the reference neutron temperature for thermal neutrons (20.46°C), and

$\sigma_a(T_o)$, $\sigma_f(T_o)$ are the absorption and fission cross section at T_o, respectively.

Combination of Equation (3.19), (3.20), and (3.21) yields

$$BU = (100) \frac{g_f(T)\ \sigma_f(T_o)}{g_a(T)\ \sigma_a(T_o)} [1 - \exp\ (\bar{\sigma}_a\ \phi_t\ C\ \tau)]. \qquad (3.22)$$

At this stage we turn back to the original problem of this section, which was to determine the fuel burnup percentages, BU, prior to refueling after 1, 2, 3, and 4 years of operation in the 1160 MW(e) HTGR.

From Appendix B

$\phi_t = 1 \times 10^{14}$ n/cm^2-sec

$c = 0.80$

$T = 890°C$

and from reference (12) for U-235

$g_f(T) = 0.9000$ for $T = 890°C$

$g_a(T) = 0.9153$

$\sigma_f(T_o) = 577.1 \times 10^{-24}$ cm^2

$\sigma_a(T_o) = 578.2 \times 10^{-24}$ cm^2.

By substituting these values in Equation (3.22) we can generate the following Table.

Table 3.3

Fuel Particle Burnups for Different Operating Times for the 1160 MW(e) HTGR.

Reactor operating time τ, years	1	2	3	4
Percent fuel burnups	42	63	73	78

Results

Equation (3.14) coupled with Equation (1.3) will make it possible to achieve the ultimate goal of this thesis, which is to find an equation describing the fuel failure percentages as a function of time following a DBDA in the 1160 MW(e) HTGR. These percentages will be computed for a burnup of 20% and for burnups prior to refueling after one, two, three, and four years of reactor operation.

Since the post-accident temperature response of the core is a function of time following a DBDA, Equation (1.3) takes the following form:

$$F(t) = \frac{100}{131 + 3.45\ BU}\ [T(t) - 1869 + 3.45\ BU], \qquad (3.23)$$

in which T(t) is given by Equation (3.14).

Equation (3.23) is the desired formula which represents the fuel failure percentage as a function of burnup and time following a DBDA in the 1160 MW(e) HTGR.

With Equation (3.23) in hand, our problem is simplified to finding fuel-failure percentages for the following five cases (see Table 3.2 for burnups):

1. Assume that the entire core is one year old at the time of the accident, which is equivalent to assuming that the fuel in the entire core has a burnup of 42%.
2. Assume that the reactor has been operated for two years at the time of the accident. This means that three quarters of the fuel in the core has a burnup of 63% and the remaining one quarter has a burnup of 42%.
3. Assume that the reactor has been operated for three years at the time of the accident. This means that 2/4, 1/4, and 1/4 of the fuel in the core have burnups of 73%, 63%, and 42%, respectively.
4. Assume that the reactor has been operated for four years at the time of the accident. This means that one quarter of the fuel in the core has a burnup of 78%, the second has a burnup of 73%, the third quarter has a burnup of 63%, and the last quarter has a burnup of 42%. This case

will correspond to the lower limit on the time required for a given percentage of fuel failure since this burnup percentage represents the maximum design burnup for the reference design HTGR.

5. Assume that the fuel in the entire core has a burnup of less than 20%. Fuel with burnups of less than 20% is assumed to have the same failure rate as the fuel with 20% burnup as was discussed in Chapter I. This case will correspond to the upper limit on the time required for a given percentage of fuel failure.

These five cases are based on the assumption that the core is designed for a four-year life time at 80% plant capacity factor. It is also assumed that a quarter of the fuel in the core is replaced each year.

Equation (3.23) makes it possible to predict some lower limits on the time required for various percentages of fuel failure following a DBDA in the 1160 MW(e) HTGR. These percentages have been computed and are shown in Figure 3.3 for burnup of 20% (case 5) and for burnups prior to refueling after one (case 1), two (case 2), three (case 3), and four (case 4) years of reactor operations. It is interesting to note that fuel particle failure in the core will not begin until after 93, 96, 101, 112, and 124 minutes in case 4, 3, 2, 1, and 5 respectively. Figure 3.3 is also an indication that after approximately 158 minutes, we will have a failure of 100 percent in

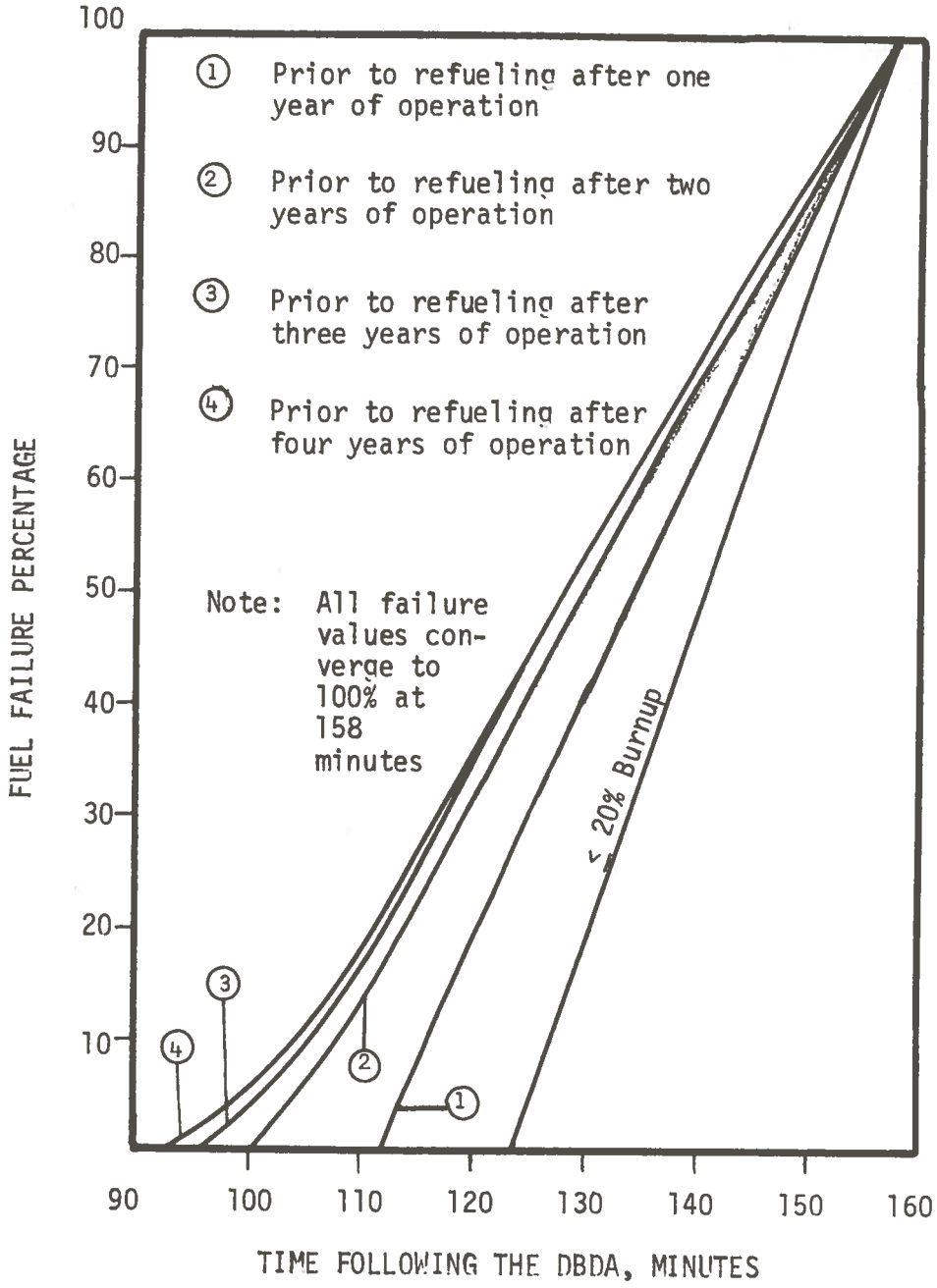

Figure 3.3. Comparison of fuel failure percentages as a function of time following the DBDA for various burnups or operating times in the 1160 MW(e) HTGR.

all cases. This means that there will be no appreciable failure for at least 93 minutes following the DBDA, and, depending upon the burnup, may require as long as 124 minutes.

The combination of the linear approximation of the post-accident temperature response of the core, Equation (3.15), and Equation (1.3) also makes it possible to estimate fuel failure percentages as a function of time following the DBDA. These percentages are shown in Figure 3.4 for each of the cases discussed in this chapter previously. A comparison of the results in Figure 3.4 with those in Figure 3.3 indicates that the values for failure computed by use of the linear approximation, Equation (3.15), are in rather good agreement with those obtained by use of the fourth-order polynomial, Equation (3.14), for low burnups. In general, failure values computed by use of the polynomial are slightly higher than those determined by use of the linear approximation. This argument implies that the results obtained through Equation (3.23) are more conservative. It should also be noted that the fourth-order polynomial estimates the "second approximation", Figure 3.1 (or Equation (2.34)), more accurately than does the linear approximation.

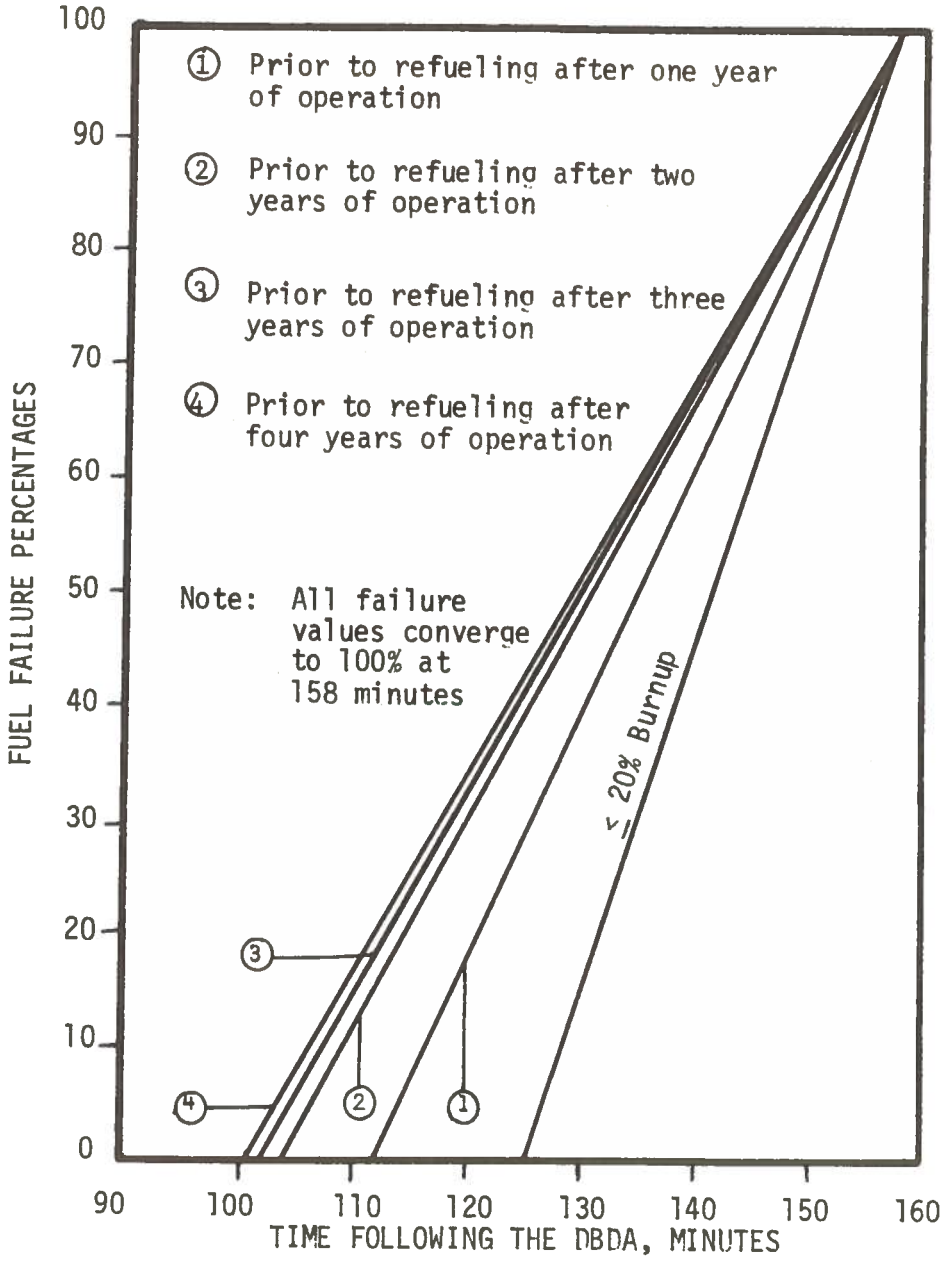

Figure 3.4. A comparison of the fuel failure percentages obtained by use of the linear-approximation for various burnups or operating times in the 1160 MW(e) HTGR.

Chapter IV

CONCLUSIONS AND RECOMMENDATIONS

Conclusions

This thesis has been an attempt to develop a method to estimate fuel particle failure percentages as a function of time following the DBDA in the HTGR. These percentages were specifically calculated for the 1160 MW(e) HTGR as an example. These results indicate that even in the absence of core cooling there will be no appreciable failure of fuel particles for at least 93 minutes following the DBDA and depending upon the burnup it may require as long as 124 minutes. In other words, in the extremely unlikely event of a DBDA followed by auxiliary circulators failure, the analysis presented here predicts that there will be at least 93 minutes before any fission products are released from the fuel. The adiabatic heat transfer model coupled with the modeling of Simith, which includes the effects of staying at temperatures for a maximum of 100 hours, makes the results obtained in this thesis very conservative.

These results are believed to represent approximate lower limits (worst case) on the time required for various percentages of fuel failure. If more realistic models are used which account for natural convection cooling and heat transfer to the reflector elements, the time lag before fuel failure is expected to be significantly larger. In fact, there may be no fuel failure at all if this cooling is sufficient to stabilize the temperature below 1600°C.

In conclusion this analysis has shown that due to the high heat capacity of the graphite core, there will be no appreciable fuel failure for at least 93 minutes following the DBDA. This delay provides valuable time to correct malfunctions and put the circulators back into operation. A major deficiency of this analysis is that it does not allow for heat transfer from the reactor fuel by convection or heat conduction to the reflector elements. In addition, the analysis fails to consider the finite time required for fission products from a failed fuel kernal to migrate to a free surface and then diffuse to the containment atmosphere.

Significance of the Study

The design of the HTGR offers a number of unique advantages in terms of safety that have not been fully recognized or allowed to impact on its design. This is because of a lack of understanding of the reactor's response to postulated accidents and the lack of independent verification of this response. In particular, more research and independent verification of the HTGR's response to a maximum hypothetical fission product release accident (i.e., a DBDA followed by a loss of emergency core cooling) is needed.

In this thesis work experience has been gained on how to accurately compute the heat generation rates from fission product decay as a function of time following the reactor shutdown. A general formula has been developed to correlate the fission product activities to the post-accident temperature response of the reactor core. This general formula makes use of a reccurence relation which greatly reduces the computer time required in the numerical computations.

In addition, a method for computing fuel failure percentages as a function of reactor burnup and time following a DBDA has been developed in this thesis.

Suggestions for Further Study

There appear to be a number of useful and significant extensions of the work contained in this thesis. Of perhaps most direct interest would be a more accurate model for determining the temperature response of the reactor core following a DBDA by accounting for core heat removal by natural convection and heat conduction to the reflector elements. This model would lead to more realistic results. It is also of importance to model the migration and subsequent diffusion of fission products following fuel failure. Then, finally by combining the two models mentioned above with fission product activities one can obtain a realistic prediction of the time dependent fission product release rates.

REFERENCES

1. Duffield, R. B., "The Development of the HTGR and the Peach Bottom Prototype," J. Brit. Nucl. Soc. 5, 305 (July 1966).

2. Walker, R. E., and T. A. Johnston, "Fort St. Vrain Nuclear Station," Nucl. Eng. Intern. 14, 1069 (Dec. 1969).

3. Dahlburg, R. C., R. F. Turner, and W. V. Goeddel, "HTGR Fuel and Fuel Cycle Summary Description," General Atomic Report GA-A12801 (Rev.), January 21, 1974.

4. Harmon, D. P., and C. B. Scott, "Development and Irradiation Performance of LHTGR Fuel," General Atomic Report GA-A13173, October 31, 1975.

5. Stansfield, O. M., "HTGR Fuel Design and Performance," General Atomic Report GA-A13072, July 12, 1974.

6. Smith, C. L., "Fuel Particle Behavior Under Normal and Transient Conditions," General Atomic Report GA-A12971, October 1, 1974.

7. Hamawi, J. H., "A Useful Recurrence Formula for the Equations of Radioactive Decay," Nuclear Technology, Vol. 11, May 1971.

8. Way, K., and E. P. Wigner, Phys. Rev. 70, 115 (1946).

9. Stehn, J. R., and E. F. Clancy, "Fission Product Radioactivity and Heat Generation," Proceedings of the Second United Nations Conference on the peaceful uses of Atomic Energy, P/1071, Vol. 13, p. 49, United Nations, New York, 1958.

10. Lamarsh, J. R., "Nuclear Reactor Theory," Second ed., Addison-Wesley Publishing Co., Reading, Massachusetts (1972).

11. Atam, A. P., "Fundamentals of Nuclear Physics," Allyn and Bacon, Inc., Boston, Massachusetts (1966).

12. Perkins, J. F., and R. W. King, "Energy Released from Fission Products," Nucl. Sci. and Eng., Vol. 3, p. 226, June 1958.

13. Weast, R. C., "Handbook of Chemistry and Physics," 48th ed., The Chemical Rubber Co., Cleveland, Ohio (1968).

14. Meek, M. E., and R. S. Gilbert, "Summary of Gamma and Beta Energy and Intensity Data," General Electric Company, NEDO-12037 (69-NED-41), Class 1, June 1970.

15. General Atomic Standard Safety Analysis Report (GASSAR 6) GA-A13200, Table 4.1-1.

APPENDICES

The appendix is divided into two parts. In Appendix A the listing of the computer program used in the analysis is presented. The computer code TEMP was used to estimate the post-accident temperature response of the core as a function of time following a design basis depressurization accident in the 1160 MW(e) HTGR. The permanent radionuclide activity and data library and the output data from this program are also included. Definitions of all symbols used in the permanent radionuclide activity and data library are given below:

ID = the isotope identification number and the file number

IP1 = the ID number of parent

IP2 = the ID number of grandparent

IPP = the ID number of second parent

BF1 = branching fraction from parent to daughter

BF2 = branching fraction from grandparent to daughter

ABE = average beta energy (MeV/disintegration)

AGE = average gamma energy (MeV/disintegration)

LAMDA = radioactive decay constant ($second^{-1}$)

DFA = design fuel activity (Curies)

DPC = design primary coolant activity (Curies)

DPA = design plateout activity (Curies)

EPC = expected primary coolant activity (Curies)

EPA = expected plateout activity (Curies).

In Appendix B, the design and performance characteristics of the 1160 MW(e) HTGR core are tabulated[15].

APPENDIX A

COMPUTER PROGRAM USED IN THE ANALYSIS

LISTING OF THE PROGRAM TEMP

```
      DIMENSION SO(2,205),ID(205),IP1(205),IP2(205),IPP(205),BF1(205),    MAIN  10
     A BF2(205),ABE(205),AGE(205),YRC(205),DFA(205),DPC(205),DPA(205),    MAIN  20
     B EPC(205),EPA(205),R(205),YRA(205),YRB(205),T(100),U(100),V(100)    MAIN  30
      REAL I1,I2,I3,I12,I23,I123                                          MAIN  40
      DEFINE FILE 8(210,20,U,ND)                                          MAIN  50
      DO 5 J=1,205                                                        MAIN  60
      ND=J                                                                MAIN  70
      READ(8'ND)  (SO(I,J),I=1,2),ID(J),IP1(J),IP2(J),IPP(J),BF1(J),      MAIN  80
     A BF2(J),ABE(J),AGE(J),YRC(J),DFA(J),DPC(J),DPA(J),EPC(J),EPA(J)     MAIN  90
      WRITE(6,10) (SO(I,J),I=1,2),ID(J),IP1(J),IP2(J),IPP(J),BF1(J),      MAIN 100
     A BF2(J),ABE(J),AGE(J),YRC(J),DFA(J),DPC(J),DPA(J),EPC(J),EPA(J)     MAIN 110
      R(J)=3.7E↑10*(ABE(J)+AGE(J))                                        MAIN 120
5     CONTINUE                                                            MAIN 130
      DO 1 J=1,205                                                        MAIN 140
      KS=ID(J)                                                            MAIN 150
      KA=IP2(KS)                                                          MAIN 160
      KB=IP1(KS)                                                          MAIN 170
      IF((KA.GT.0).AND.(KB.GT.0))  GO TO 3                                MAIN 180
      IF(KB.GT.0) GO TO 2                                                 MAIN 190
      YRA(J)=0.0                                                          MAIN 200
      YRB(J)=0.0                                                          MAIN 210
      GO TO 4                                                             MAIN 220
2     YRA(J)=0.0                                                          MAIN 230
      YRB(J)=YRC(KB)                                                      MAIN 240
      GO TO 4                                                             MAIN 250
3     YRA(J)=YRC(KA)                                                      MAIN 260
      YRB(J)=YRC(KB)                                                      MAIN 270
4     CONTINUE                                                            MAIN 280
1     CONTINUE                                                            MAIN 290
10    FORMAT(2A4,2X,4I5,0PF7.2,3F7.2,1PE12.3,5E10.2)                      MAIN 300
      TO=752.0                                                            MAIN 310
      CPM=0.172*1.062E+05+0.0331*9500.0+0.0276*440.0                      MAIN 320
      C1=3.827E-14/(CPM*3944.0)                                           MAIN 330
      DO 20 I=1,100                                                       MAIN 340
      PA=0.0                                                              MAIN 350
      PB=0.0                                                              MAIN 360
```

```
      PC=0.0                                                                    MAIN 370
      DO 15 J=1,205                                                             MAIN 380
      TT=I-1                                                                    MAIN 390
      IF(YRC(J).EQ.0.0) YRC(J)=1.0E-19                                          MAIN 400
      IF(YRB(J).EQ.0.0) YRB(J)=1.0E-20                                          MAIN 410
      IF(YRA(J).EQ.0.0) YRA(J)=1.0E-21                                          MAIN 420
      W=YRC(J)*TT*15.0*60.0                                                     MAIN 430
      W1=YRB(J)*TT*15.0*60.0                                                    MAIN 440
      W2=YRA(J)*TT*15.0*60.0                                                    MAIN 450
      I1=(1.0-EXP(-W2))/YRA(J)                                                  MAIN 460
      I2=(1.0-EXP(-W1))/YRB(J)                                                  MAIN 470
      I3=(1.0-EXP( -W))/YRC(J)                                                  MAIN 480
      I12=(I1-I2)/(YRB(J)-YRA(J))                                               MAIN 490
      I23=(I2-I3)/(YRC(J)-YRB(J))                                               MAIN 500
      I123=(I1-I3)/(YRC(J)-YRA(J))                                              MAIN 510
      C=R(J)*DFA(J)*I3                                                          MAIN 520
      B=R(J)*(YRC(J)*DFA(IP1(J))*I23+DFA(J)*I3)                                 MAIN 530
      A=R(J)*(YRC(J)*(YRB(J)*DFA(IP2(J))*I123+DFA(IP1(J))*I23)                  MAIN 540
     1 +DFA(J)*I3)                                                              MAIN 550
      PC=PC+C                                                                   MAIN 560
      PB=PB+B                                                                   MAIN 570
      PA=PA+A                                                                   MAIN 580
15    CONTINUE                                                                  MAIN 590
      T(I)=TO+C1*PC                                                             MAIN 600
      U(I)=TO+C1*PB                                                             MAIN 610
      V(I)=TO+C1*PA                                                             MAIN 620
20    CONTINUE                                                                  MAIN 630
      WRITE(6,25) (T(I),I=1,100)                                                MAIN 640
      WRITE(6,30)                                                               MAIN 650
      WRITE(6,25) (U(I),I=1,100)                                                MAIN 660
25    FORMAT(1PE10.3,11E10.3)                                                   MAIN 670
30    FORMAT(// '  SECOND APPROXIMATION',//)                                   MAIN 680
      WRITE(6,35)                                                               MAIN 690
35    FORMAT(//  '  THIRD APPROXIMATION',//)                                   MAIN 700
      WRITE(6,25) (V(I),I=1,100)                                                MAIN 710
      STOP                                                                      MAIN 720
      END                                                                       MAIN 730
```

********** PERMANENT RADIONUCLIDE ACTIVITY AND DATA LIBRARY **********

ISOTOPE	ID	IP1	IP2	IPP	BF1	BF2	ABE	AGE	LAMBDA	DFA	DPC	DPA	EPC	EPA
H-3	1	0	0	0	1.00	0.0	0.00	0.0	1.790E-09	3.43E+04	5.87E+00	0.0	4.15E+00	0.0
N-13	2	0	0	0	1.00	0.0	0.0	0.0	1.160E-03	0.0	0.0	0.0	0.0	0.0
C-14	3	0	0	0	1.00	0.0	0.05	0.0	3.840E-12	2.69E+03	0.0	0.0	0.0	0.0
N-16	4	0	0	0	1.00	0.0	1.94	4.62	9.630E-02	0.0	0.0	0.0	0.0	0.0
F-18	5	0	0	0	1.00	0.0	0.0	0.0	1.050E-02	0.0	0.0	0.0	0.0	0.0
O-19	6	0	0	0	1.00	0.0	1.14	0.98	2.390E-02	0.0	0.0	0.0	0.0	0.0
NA-24	7	0	0	0	1.00	0.0	0.55	0.0	1.280E-05	0.0	0.0	0.0	0.0	0.0
P-32	8	0	0	0	1.00	0.0	0.69	0.0	5.610E-07	0.0	0.0	0.0	0.0	0.0
A-41	9	0	0	0	1.00	0.0	0.40	1.28	1.050E-04	0.0	0.0	0.0	0.0	0.0
SC-46M	10	0	0	0	1.00	0.0	0.0	0.0	3.470E-02	0.0	0.0	0.0	0.0	0.0
SC-46	11	10	0	0	1.00	0.0	0.11	0.0	9.560E-08	0.0	0.0	0.0	0.0	0.0
V-48	12	0	0	0	1.00	0.0	0.0	0.0	5.010E-07	0.0	0.0	0.0	0.0	0.0
CR-51	13	0	0	0	1.00	0.0	0.0	0.0	2.890E-07	0.0	0.0	0.0	0.0	0.0
MN-54	14	0	0	0	1.00	0.0	0.0	0.0	2.650E-08	0.0	0.0	0.0	0.0	0.0
MN-56	15	0	0	0	1.00	0.0	0.86	0.0	7.470E-05	0.0	0.0	0.0	0.0	0.0
FE-55	16	0	0	0	1.00	0.0	0.0	0.0	8.450E-09	0.0	0.0	0.0	0.0	0.0
FE-59	17	0	0	0	1.00	0.0	0.12	0.0	1.780E-07	0.0	0.0	0.0	0.0	0.0
CO-58M	18	0	0	0	1.00	0.0	0.0	0.0	2.140E-05	0.0	0.0	0.0	0.0	0.0
CO-58	19	18	0	0	1.00	0.0	0.0	0.0	1.130E-07	0.0	0.0	0.0	0.0	0.0
CO-60M	20	0	0	0	1.00	0.0	0.60	0.0	1.130E-03	0.0	0.0	0.0	0.0	0.0
CO-60	21	20	0	0	1.00	0.0	0.09	0.0	4.160E-09	0.0	0.0	0.0	0.0	0.0
CU-64	22	0	0	0	1.00	0.0	0.19	0.0	1.550E-05	0.0	0.0	0.0	0.0	0.0
CU-66	23	0	0	0	1.00	0.0	1.06	0.0	2.270E-03	0.0	0.0	0.0	0.0	0.0
NI-65	24	0	0	0	1.00	0.0	0.67	0.0	7.520E-05	0.0	0.0	0.0	0.0	0.0
ZN-65	25	0	0	0	1.00	0.0	0.0	0.0	4.720E-08	0.0	0.0	0.0	0.0	0.0
ZN-69M	26	0	0	0	1.00	0.0	0.0	0.0	1.400E-05	0.0	0.0	0.0	0.0	0.0
ZN-69	27	26	0	0	1.00	0.0	0.32	0.0	2.030E-04	0.0	0.0	0.0	0.0	0.0
GE-79	28	0	0	0	1.00	0.0	0.0	0.0	1.160E-02	4.87E+06	3.99E+01	4.87E+01	3.51E-02	3.51E-01
AS-79	29	28	0	0	1.00	0.0	0.94	0.03	1.280E-03	4.98E+06	3.01E+01	9.85E+01	4.65E-03	7.09E-01
SE-79M	30	29	28	0	1.00	0.0	0.0	0.01	2.960E-03	4.98E+06	2.17E+02	4.71E+02	8.13E-01	2.92E+01
SE-81	31	0	0	0	1.00	0.0	0.46	0.15	6.420E-04	8.49E+06	0.0	1.27E+03	7.79E-01	1.23E+02
SE-83M	32	0	0	0	1.00	0.0	1.40	0.15	9.900E-03	1.56E+07	0.0	7.01E+02	4.97E+00	5.49E+01
SE-83	33	0	0	0	1.00	0.0	0.58	1.13	5.020E-04	9.82E+06	2.72E+02	1.65E+03	7.77E-01	1.57E+02
SE-84	34	0	0	0	1.00	0.0	0.71	0.30	3.610E-03	4.39E+07	1.77E+03	3.02E+03	9.06E+00	2.62E+02
BR-83	35	33	32	32	1.00	0.0	0.30	0.01	7.990E-05	2.54E+07	3.39E+02	1.26E+04	8.09E-01	1.22E+03
BR-84	36	34	0	0	1.00	0.0	0.95	2.36	3.630E-04	4.44E+07	1.31E+03	1.17E+04	9.06E+00	1.10E+03
BR-85	37	0	0	0	1.00	0.0	0.60	0.0	3.850E-03	5.92E+07	2.38E+03	3.95E+03	1.24E+01	3.36E+02
BR-87	38	0	0	0	1.00	0.0	1.22	2.40	1.260E-02	0.0	0.0	0.0	0.0	0.0
KR-83M	39	35	33	0	1.00	0.0	0.03	0.00	1.040E-04	2.54E+07	1.54E+04	0.0	1.50E+03	0.0
KR-85M	40	37	0	0	1.00	0.0	0.10	0.16	4.380E-05	5.91E+07	1.83E+04	0.0	1.81E+03	0.0
KR-85	41	40	37	0	0.23	0.0	0.23	0.00	2.040E-09	1.47E+06	3.50E+01	0.0	2.93E+00	0.0
KR-87	42	38	0	0	1.00	0.0	1.01	0.86	1.520E-04	8.27E+07	1.91E+04	0.0	2.05E+03	0.0
KR-88	43	0	0	0	1.00	0.0	0.31	2.00	6.880E-05	1.47E+08	3.94E+04	0.0	4.09E+03	0.0
KR-89	44	0	0	0	1.00	0.0	1.00	2.22	3.530E-03	1.35E+08	9.18E+03	0.0	9.31E+02	0.0
KR-90	45	0	0	0	1.00	0.0	0.82	2.10	2.150E-02	1.29E+08	4.38E+03	0.0	3.54E+02	0.0
KR-91	46	0	0	0	1.00	0.0	1.85	0.16	8.080E-02	8.70E+07	1.93E+03	0.0	9.34E+01	0.0
RB-88	47	43	0	0	1.00	0.0	1.40	0.90	6.530E-04	1.49E+08	8.36E+04	4.09E+04	2.64E+01	4.10E+03
RB-89	48	44	0	0	1.00	0.0	0.73	2.40	7.600E-04	1.51E+08	2.45E+03	1.07E+04	7.07E+00	9.45E+02
RB-90M	49	45	0	0	1.00	0.0	0.0	0.0	2.700E-03	2.89E+07	1.49E+02	2.89E+02	5.56E-02	2.13E+00
RB-90	50	49	45	0	1.00	0.0	1.12	3.64	4.280E-03	1.71E+08	3.91E+03	6.38E+03	1.51E+01	3.72E+02
RB-91	51	46	0	0	1.00	0.0	1.50	0.0	1.200E-02	1.49E+08	2.82E+03	3.42E+03	1.14E+01	1.07E+02
SR-89	52	48	44	0	1.00	0.0	0.49	0.0	1.580E-07	1.53E+08	2.48E-01	1.22E+04	3.36E-05	9.60E+02
SR-90	53	50	49	0	1.00	0.0	0.18	0.0	7.610E-10	8.09E+06	7.86E-03	1.54E+04	5.50E-05	4.10E+03

SR-91	54	51	46	0	1.00	0.0	0.54	0.70	1.900E-05	1.53E+06	3.30E+01	4.95E+03	5.20E-03	1.22E+02
SR-92	55	0	0	0	1.00	0.0	0.21	1.26	7.160E-05	1.68E+08	4.60E+01	1.68E+03	1.17E-02	1.65E+01
SR-93	56	0	0	0	1.00	0.0	1.26	1.47	1.540E-03	1.69E+08	6.37E+02	1.69E+03	2.43E-01	1.62E+01
SR-94	57	0	0	0	1.00	0.0	0.70	1.42	8.960E-03	1.61E+08	1.25E+03	1.61E+03	1.05E+00	1.29E+01
Y-90	58	53	50	0	1.00	0.0	0.93	0.0	3.010E-06	8.09E+06	9.56E-02	1.55E+04	2.33E-05	4.10E-03
Y-90M	59	54	51	0	0.50	0.0	0.02	0.52	2.290E-04	9.37E+07	7.91E+01	3.96E+03	2.07E-02	8.35E-01
Y-91	60	59	54	54	1.00	0.41	0.51	0.60	1.360E-07	1.53E+08	8.80E-02	7.48E+03	2.04E-05	1.58E+02
Y-92	61	55	0	0	1.00	0.0	1.13	0.24	5.450E-05	1.72E+08	3.71E+01	3.40E+03	9.04E-03	3.32E+01
Y-93	62	56	0	0	1.00	0.0	0.93	0.05	1.890E-05	1.83E+08	1.82E+01	3.52E+03	3.38E-03	3.40E+01
Y-94	63	57	0	0	1.00	0.0	1.42	0.74	8.210E-04	1.72E+08	5.43E+02	3.33E+03	1.02E-01	3.01E+01
Y-95	64	0	0	0	1.00	0.0	0.0	0.0	1.100E-03	1.73E+08	5.23E+02	1.73E+03	1.78E-01	1.65E+01
Y-96	65	0	0	0	1.00	0.0	0.0	0.0	5.020E-03	1.59E+08	1.05E+03	1.59E+03	6.44E-01	1.36E+01
ZR-95	66	64	0	0	1.00	0.0	0.13	0.73	1.230E-07	1.72E+08	1.09E-01	3.47E+03	2.07E-05	3.34E+01
ZR-97	67	0	0	0	1.00	0.0	0.75	0.04	1.150E-05	1.59E+08	7.12E+00	1.59E+03	1.70E-03	1.50E+01
NB-95M	68	66	64	0	0.02	0.0	0.16	0.07	2.210E-06	2.24E+06	1.95E-02	6.76E+01	4.83E-05	6.55E-01
NB-95	69	68	66	66	1.00	0.98	0.05	0.76	2.290E-07	1.72E+08	1.55E-01	5.21E+03	3.79E-05	5.04E+01
NB-97M	70	67	0	0	1.00	0.0	0.0	0.75	1.150E-02	0.0	0.0	0.0	0.0	0.0
NB-97	71	70	67	0	1.00	0.0	0.47	0.67	1.570E-04	1.59E+08	9.30E+01	3.18E+03	2.35E-02	3.01E+01
NB-98	72	0	0	0	1.00	0.0	0.0	2.05	2.270E-04	5.86E+06	4.80E+00	5.86E+01	9.47E-04	4.23E-01
NB-99M	73	0	0	0	1.00	0.0	0.0	0.0	4.440E-03	5.03E+07	3.20E+02	5.03E+02	1.99E-01	4.71E+00
NB-99	74	73	0	0	1.00	0.0	0.00	1.36	4.950E-02	1.04E+08	9.86E+02	1.04E+03	3.11E+00	9.45E+00
NB-100M	75	0	0	0	1.00	0.0	1.45	0.0	9.630E-04	8.33E+07	2.29E+02	8.33E+02	6.39E-02	6.75E+00
NB-100	76	75	0	0	1.00	0.0	0.0	0.86	3.980E-03	8.33E+07	5.08E+02	8.33E+02	2.57E-01	6.75E+00
MO-99	77	74	73	0	1.00	0.0	0.40	0.13	2.810E-06	1.64E+08	3.34E+00	3.18E+03	5.14E-04	2.88E+01
MO-101	78	0	0	0	1.00	0.0	0.42	1.66	7.910E-04	1.37E+08	3.24E+02	1.37E+03	8.24E-02	1.06E+01
MO-102	79	0	0	0	1.00	0.0	0.44	0.0	1.040E-03	1.13E+08	3.27E+02	1.13E+03	8.53E-02	8.35E+00
MO-103M	80	0	0	0	1.00	0.0	0.0	2.25	3.630E-05	1.18E+07	1.66E+00	1.18E+02	4.13E-04	1.15E+00
MO-103	81	80	0	0	1.00	0.0	0.0	0.0	1.050E-02	7.63E+07	6.15E+02	8.22E+02	5.18E-01	6.07E+00
MO-104	82	0	0	0	1.00	0.0	0.0	0.0	8.890E-03	4.71E+07	3.66E+02	4.77E+02	2.70E-01	3.33E+00
MO-105	83	0	0	0	1.00	0.0	0.0	0.0	1.730E-02	0.0	0.0	0.0	0.0	0.0
TC-99M	84	77	74	0	0.88	0.0	0.0	0.13	3.210E-05	1.45E+08	1.80E+01	4.24E+03	4.09E-03	3.82E+01
TC-101	85	78	0	0	1.00	0.0	0.48	0.35	8.140E-04	1.37E+08	4.10E+02	2.73E+03	8.54E-02	2.12E+01
TC-104	86	82	0	0	1.00	0.0	0.98	1.93	6.420E-04	4.80E+07	1.73E+02	9.61E+02	2.45E-02	6.93E+00
TC-105	87	83	0	0	1.00	0.0	0.68	1.30	1.480E-03	2.23E+07	8.21E+01	2.23E+02	1.66E-02	1.14E+00
RU-103	88	81	80	0	1.00	0.0	0.06	0.50	2.020E-07	8.31E+07	1.15E-01	1.71E+03	1.35E-05	1.29E+01
RU-105	89	87	83	0	1.00	0.0	0.41	0.73	4.370E-05	2.54E+07	5.63E+00	4.77E+02	5.53E-04	2.41E+00
RU-106	90	0	0	0	1.00	0.0	0.01	0.0	2.180E-08	7.30E+06	8.98E-04	1.05E+02	1.79E-07	8.30E-01
RU-107	91	0	0	0	1.00	0.0	0.96	0.22	2.750E-03	5.11E+06	2.66E+01	5.11E+01	1.04E-02	3.93E-01
RH-103M	92	88	81	0	0.99	0.0	0.04	0.00	2.100E-04	8.21E+07	6.26E+01	2.52E+03	1.28E-02	1.89E+01
RH-105	93	89	87	0	1.00	0.0	0.15	0.10	5.420E-06	2.15E+07	5.52E-01	7.30E+02	6.83E-05	3.60E+00
RH-106	94	90	0	0	1.00	0.0	1.36	0.33	2.310E-02	0.0	0.0	0.0	0.0	0.0
RH-107	95	91	0	0	1.00	0.0	0.40	0.39	5.160E-04	5.11E+06	1.31E+01	1.02E+02	2.06E-03	7.87E-01
AG-105	96	0	0	0	1.00	0.0	0.0	0.0	2.010E-07	0.0	0.0	0.0	0.0	0.0
AG-110M	97	0	0	0	1.00	0.0	0.07	2.79	3.170E-08	1.72E+03	4.01E-02	3.21E+03	1.01E-04	3.21E+02
AG-110	98	97	0	0	0.01	0.0	1.18	0.05	2.840E-02	0.0	0.0	0.0	0.0	0.0
CD-107	99	0	0	0	1.00	0.0	0.0	0.0	2.960E-05	0.0	0.0	0.0	0.0	0.0
IN-114M	100	0	0	0	1.00	0.0	0.0	0.0	1.610E-08	0.0	0.0	0.0	0.0	0.0
IN-114	101	100	0	0	0.95	0.0	0.78	0.0	9.630E-03	0.0	0.0	0.0	0.0	0.0
IN-115	102	0	0	0	1.00	0.0	1.35	2.51	4.950E-02	0.0	0.0	0.0	0.0	0.0
SN-119M	103	0	0	0	1.00	0.0	0.0	0.01	3.270E-08	1.31E+04	2.08E-06	1.61E-01	3.82E-10	1.18E-03
SN-123	104	0	0	0	1.00	0.0	0.45	0.01	6.220E-08	4.05E+05	1.30E-04	1.14E+00	2.85E-08	4.68E-02
SN-125	105	0	0	0	1.00	0.0	0.91	0.28	8.310E-07	1.26E+06	4.19E-03	1.28E+01	6.92E-07	8.39E-02
SN-127M	106	0	0	0	1.00	0.0	0.0	0.50	2.750E-03	6.27E+06	3.26E+01	6.27E+01	1.23E-02	4.64E-01
SN-127	107	106	0	0	1.00	0.0	0.43	2.00	9.080E-05	6.27E+06	2.16E+00	6.27E+01	3.63E-04	4.03E-01
SN-128	108	0	0	0	1.00	0.0	0.47	0.0	1.950E-04	1.80E+07	1.29E+01	1.80E+02	2.76E-03	1.42E+00
SN-129M	109	0	0	0	1.00	0.0	0.0	0.0	5.780E-03	1.10E+07	7.69E+01	1.10E+02	5.80E-02	1.07E+00
SN-129	110	109	0	0	1.00	0.0	0.0	0.0	1.540E-03	1.10E+07	4.16E+01	1.10E+02	1.29E-02	6.55E-01
SN-130	111	0	0	0	1.00	0.0	0.78	0.0	4.440E-03	2.89E+07	1.84E+02	2.89E+02	9.69E-02	2.30E+00
SN-131	112	0	0	0	1.00	0.0	0.0	0.0	8.900E-03	2.63E+07	1.35E+02	2.63E+02	1.99E-01	1.72E+00
SN-132	113	0	0	0	1.00	0.0	0.0	0.0	1.160E-02	2.53E+07	2.07E+02	2.53E+02	1.37E-01	1.33E+00
SB-125	114	105	0	0	1.00	0.0	0.08	0.55	8.050E-03	1.17E+06	1.35E-03	4.40E+02	8.22E-06	1.03E+02
SB-127	115	107	106	0	1.00	0.0	0.37	0.51	2.110E-06	1.58E+07	1.60E-01	2.63E+02	2.27E-05	1.94E+00
SB-128M	116	108	0	0	1.00	0.0	0.35	1.84	1.110E-03	2.22E+07	7.13E+01	3.97E+02	1.86E-02	3.09E+00

SB-128	117	112	108	0	0.97	0.0	1.20	1.07	2.140E-05	5.25E+06	4.41E-01	5.79E-01	7.82E-05	4.11E-01
SB-129	118	113	109	0	1.00	0.0	0.85	0.0	4.440E-05	4.36E+07	9.51E+00	6.57E+02	1.49E-03	5.24E+00
SB-130M	119	114	0	0	1.00	0.0	0.73	0.0	1.440E-03	1.84E+07	6.65E+01	1.84E+02	2.20E-02	1.56E+00
SB-130	120	119	111	0	1.00	0.0	1.20	2.67	3.120E-04	4.04E+07	5.43E+01	6.93E+02	1.22E-02	6.15E+00
SB-131	121	117	0	0	1.00	0.0	0.85	1.02	5.020E-04	6.13E+07	1.35E+02	8.76E+02	3.09E-02	7.81E+00
SB-132	122	118	0	0	1.00	0.0	2.15	1.60	3.730E-03	7.44E+07	5.60E+02	9.97E+02	2.15E-01	7.21E+00
SB-133	123	0	0	0	1.00	0.0	0.78	2.46	4.280E-03	9.68E+07	5.44E+02	8.68E+02	2.40E-01	5.90E+00
SB-134	124	0	0	0	1.00	0.0	0.0	0.0	6.130E-02	0.0	0.0	0.0	0.0	0.0
TE-125M	125	114	105	0	1.00	0.0	0.0	0.00	1.380E-07	2.45E+05	4.05E-02	8.38E-02	8.38E-05	8.28E-01
TE-127M	126	115	107	0	0.16	0.0	0.09	0.00	7.300E-07	2.59E+06	3.23E+01	1.12E+04	7.50E-04	1.03E+03
TE-127	127	126	115	115	0.99	0.84	0.22	0.00	2.070E-05	1.57E+07	3.30E+01	1.54E+04	6.77E-02	1.35E+03
TE-129M	128	116	110	0	1.00	0.0	0.24	0.05	2.350E-07	7.65E+06	1.70E+00	1.85E+04	3.78E-03	1.62E+03
TE-129	129	126	118	0	0.64	0.0	0.45	0.12	1.670E-04	4.26E+07	2.58E+02	1.66E+04	5.67E-01	1.35E+03
TE-131M	130	121	112	0	0.15	0.0	0.20	1.44	6.420E-06	2.35E+07	2.72E+01	1.08E+04	6.07E-02	9.54E+02
TE-131	131	130	121	0	0.18	0.85	0.74	0.50	4.620E-04	7.07E+07	7.04E+02	7.21E+03	2.03E+00	5.23E+02
TE-132	132	122	113	0	1.00	0.0	0.19	0.24	2.470E-06	1.18E+08	8.51E+01	8.82E+04	2.46E-01	1.01E+04
TE-133M	133	123	0	0	0.72	0.0	0.19	0.27	2.180E-04	1.12E+08	8.03E+02	1.04E+04	1.90E+00	8.83E+02
TE-133	134	133	130	0	0.13	0.28	0.62	1.90	9.240E-04	7.50E+07	1.01E+03	5.14E+03	3.07E+00	4.54E+02
TE-134	135	124	0	0	1.00	0.0	0.51	0.0	2.690E-04	1.71E+08	1.30E+03	1.36E+04	2.98E+00	1.12E+03
I-129	136	128	129	129	1.00	0.36	0.06	0.02	1.290E-15	0.0	0.0	3.33E+00	2.60E-09	2.67E+01
I-131	137	131	130	130	1.00	0.82	0.21	0.38	9.950E-07	9.04E+07	4.11E+01	1.20E+05	1.13E-01	1.29E+04
I-132	138	132	122	0	1.00	0.0	0.42	2.29	8.430E-05	1.27E+08	5.49E+02	1.05E+05	1.51E+00	1.19E+04
I-133	139	134	133	0	1.00	0.87	0.40	0.64	9.260E-06	1.81E+08	2.58E+02	8.37E+04	6.98E-01	8.82E+03
I-134	140	135	124	0	1.00	0.0	0.56	2.51	2.210E-04	1.92E+08	1.43E+03	3.02E+04	3.54E+00	2.74E+03
I-135	141	0	0	0	1.00	0.0	0.47	1.46	2.870E-05	1.71E+08	4.26E+02	3.81E+04	1.06E+00	3.72E+03
I-136	142	0	0	0	1.00	0.0	0.84	2.77	8.150E-03	9.34E+07	1.60E+03	2.09E+03	7.40E+00	9.89E+01
XE-131M	143	137	131	0	0.01	0.0	0.13	0.02	6.710E-07	5.42E+05	2.30E+01	0.0	2.50E+00	0.0
XE-133M	144	139	134	0	0.02	0.0	0.19	0.02	3.540E-06	5.06E+06	4.19E+02	0.0	4.56E+01	0.0
XE-133	145	144	139	139	1.00	0.98	0.13	0.07	1.520E-06	1.81E+08	8.65E+03	0.0	9.39E+02	0.0
XE-135M	146	141	0	0	0.30	0.0	0.09	0.44	7.360E-04	2.81E+07	6.70E+03	0.0	6.49E+02	0.0
XE-135	147	146	141	141	1.00	0.70	0.30	0.25	2.100E-05	2.09E+07	1.61E+04	0.0	1.59E+03	0.0
XE-137	148	0	0	0	1.00	0.0	1.37	0.19	3.020E-03	1.59E+08	4.79E+03	0.0	3.92E+02	0.0
XE-138	149	0	0	0	1.00	0.0	0.56	0.93	8.140E-04	1.67E+08	7.91E+03	0.0	7.06E+02	0.0
XE-139	150	0	0	0	1.00	0.0	1.52	0.46	1.730E-02	1.33E+08	2.44E+03	0.0	1.06E+02	0.0
XE-140	151	0	0	0	1.00	0.0	1.05	1.54	5.100E-02	1.03E+08	1.52E+03	0.0	3.83E+01	0.0
XE-141	152	0	0	0	1.00	0.0	0.0	0.0	3.470E-01	0.0	0.0	0.0	0.0	0.0
CS-134M	153	0	0	0	1.00	0.0	0.0	0.0	6.640E-05	0.0	0.0	0.0	0.0	0.0
CS-134	154	153	0	0	1.00	0.0	0.15	1.60	1.070E-08	1.50E+07	2.43E-01	5.78E+04	6.45E-04	6.10E+03
CS-136	155	0	0	0	1.00	0.0	0.11	2.16	6.170E-07	1.07E+07	2.60E-02	1.07E+02	6.55E-06	1.07E+00
CS-137	156	148	0	0	1.00	0.0	0.55	0.0	7.280E-10	7.83E+06	8.77E-02	1.59E+05	2.25E-04	1.62E+04
CS-138	157	149	0	0	1.00	0.0	0.90	2.15	3.590E-04	1.80E+08	1.20E+03	9.71E+03	2.67E+00	7.24E+02
CS-139	158	150	0	0	1.00	0.0	1.24	0.20	1.240E-03	1.74E+08	1.37E+03	4.18E+03	1.49E+00	1.23E+02
CS-140	159	151	0	0	1.00	0.0	1.47	1.59	1.000E-02	1.56E+08	2.49E+03	3.08E+03	5.13E+00	5.27E+01
BA-137M	160	156	148	0	0.93	0.0	0.06	0.60	4.530E-03	7.23E+06	4.63E+01	1.49E+05	3.04E-02	1.52E+04
BA-139	161	158	150	0	1.00	0.0	0.78	0.04	1.390E-04	1.76E+08	1.62E+02	5.95E+03	2.52E-02	1.40E+02
BA-140	162	159	151	0	1.00	0.0	0.28	0.21	6.270E-07	1.69E+08	1.03E+00	4.76E+03	1.35E-04	6.93E+01
BA-141	163	0	0	0	1.00	0.0	0.77	0.63	6.310E-04	1.56E+08	3.10E+02	1.56E+03	9.54E-02	1.53E+01
BA-142	164	0	0	0	1.00	0.0	0.0	2.12	1.060E-03	1.42E+08	4.25E+02	1.42E+03	1.50E-01	1.42E+01
LA-140	165	162	159	0	1.00	0.0	0.54	2.34	4.790E-06	1.63E+08	3.12E+00	6.46E+03	7.90E-04	8.60E+01
LA-141	166	163	0	0	1.00	0.0	0.80	0.03	4.960E-05	1.59E+08	3.64E+01	3.14E+03	7.84E-03	3.11E+01
LA-142	167	164	0	0	1.00	0.0	0.73	2.36	1.250E-04	1.75E+08	1.02E+02	3.18E+03	2.04E-02	3.05E+01
LA-143	168	0	0	0	1.00	0.0	1.10	0.64	8.250E-04	1.58E+08	3.82E+02	1.56E+03	1.25E-01	1.54E+01
CE-141	169	166	163	0	1.00	0.0	0.18	0.08	2.470E-07	1.58E+08	1.57E-01	4.73E+03	3.87E-05	4.69E+01
CE-143	170	168	0	0	1.00	0.0	0.39	0.31	5.830E-06	1.59E+08	4.52E+00	3.15E+03	9.25E-04	3.13E+01
CE-144	171	0	0	0	1.00	0.0	0.11	0.02	2.620E-06	1.07E+08	1.54E-02	1.39E+03	3.65E-06	1.31E+01
CE-145	172	0	0	0	1.00	0.0	0.51	0.90	3.980E-03	1.66E+08	6.46E+02	1.06E+03	3.63E-01	9.55E+00
CE-146	173	0	0	0	1.00	0.0	0.22	0.37	8.140E-04	7.84E+07	1.90E+02	7.85E+02	5.33E-02	6.66E+00
CE-147	174	0	0	0	1.00	0.0	0.0	0.0	9.900E-03	5.38E+07	4.28E+02	5.38E+02	3.55E-01	3.97E+00
PR-143	175	170	168	0	1.00	0.0	0.31	0.0	5.910E-07	1.59E+08	3.71E-01	4.74E+03	9.31E-05	4.72E+01
PR-144	176	171	0	0	1.00	0.0	0.99	0.03	6.680E-04	1.07E+08	1.54E+02	2.46E+03	6.65E-02	2.32E+01
PR-145	177	172	0	0	1.00	0.0	0.64	0.05	3.320E-05	1.66E+08	2.13E+01	2.12E+03	3.21E-03	1.93E+01
PR-146	178	173	0	0	1.00	0.0	1.25	1.11	4.770E-04	8.03E+07	1.57E+02	1.59E+03	3.46E-02	1.39E+01
PR-147	179	174	0	0	1.00	0.0	0.0	0.08	9.630E-04	6.02E+07	2.83E+02	1.14E+03	5.39E-02	9.32E+00

PR-148	180	0	0	0	1.00	0.0	0.0	0.0	5.780E-03	4.47E+07	3.10E+02	4.47E+02	1.97E-01	3.64E+00
PR-149	181	0	0	0	1.00	0.0	0.0	0.01	5.020E-03	2.66E+07	1.76E+02	2.65E+02	9.10E-02	1.92E+00
ND-147	182	179	174	0	1.00	0.0	0.27	0.14	7.250E-07	6.05E+07	2.53E-01	1.75E+03	3.94E-05	1.47E+01
ND-149	183	181	0	0	1.00	0.0	0.45	0.33	1.110E-04	2.86E+07	1.94E+01	5.51E+02	2.71E-03	4.28E+00
ND-151	184	0	0	0	1.00	0.0	0.72	1.24	9.320E-04	1.00E+07	2.90E+01	1.08E+02	7.78E-03	8.50E-01
ND-152	185	0	0	0	1.00	0.0	0.0	0.0	9.870E-04	5.78E+06	1.62E+01	5.78E+01	3.68E-03	3.80E-01
PM-147	186	182	179	0	1.00	0.0	0.06	0.0	8.400E-09	1.85E+07	1.99E-03	2.35E+03	4.50E-07	2.02E+01
PM-148M	187	180	0	0	1.00	0.0	0.15	1.32	1.930E-07	1.90E+06	1.45E-03	1.90E+01	3.64E-07	1.90E-01
PM-148	188	187	180	0	0.07	0.0	0.68	0.62	1.490E-06	8.03E+06	4.69E-02	8.03E+01	1.18E-05	8.03E-01
PM-149	189	183	181	0	1.00	0.0	0.36	0.28	3.630E-05	2.82E+07	4.36E-01	8.38E+02	8.55E-05	6.66E+00
PM-151	190	184	0	0	1.00	0.0	0.38	0.45	6.780E-06	1.13E+07	3.78E-01	2.21E+02	6.70E-05	1.84E+00
PM-152	191	185	0	0	1.00	0.0	0.86	0.0	2.750E-03	7.07E+06	4.51E+01	1.29E+02	1.55E-02	9.60E-01
PM-153	192	0	0	0	1.00	0.0	0.61	0.0	2.100E-03	3.91E+06	1.77E+01	3.91E+01	5.92E-03	2.90E-01
SM-151	193	190	184	0	1.00	0.0	0.02	0.02	2.360E-10	3.93E+03	1.47E-04	3.83E+02	1.14E-06	1.04E+02
SM-153	194	192	0	0	1.00	0.0	0.23	0.04	4.110E-06	2.48E+06	9.39E-02	7.95E+01	1.35E-05	6.16E-01
EU-152	195	191	185	0	1.00	0.0	0.29	1.02	1.570E-09	1.00E+02	9.25E-08	1.19E-01	8.16E-10	4.17E-02
EU-154	196	0	0	0	1.00	0.0	0.23	1.22	2.820E-09	4.72E+04	4.57E-05	3.88E+01	4.03E-07	1.36E+01
EU-155	197	0	0	0	1.00	0.0	0.04	0.0	4.400E-09	1.64E+04	1.68E-05	9.63E+00	1.49E-07	3.37E+00
HF-175	198	0	0	0	1.00	0.0	0.0	0.0	1.150E-07	0.0	0.0	0.0	0.0	0.0
HF-181	199	0	0	0	1.00	0.0	0.12	0.0	1.890E-07	0.0	0.0	0.0	0.0	0.0
TA-182M	200	0	0	0	1.00	0.0	0.0	0.0	7.000E-04	0.0	0.0	0.0	0.0	0.0
TA-182	201	200	0	0	1.00	0.0	0.09	0.0	6.980E-08	0.0	0.0	0.0	0.0	0.0
TA-185	202	0	0	0	1.00	0.0	0.62	0.0	2.310E-04	0.0	0.0	0.0	0.0	0.0
W-185M	203	0	0	0	1.00	0.0	0.0	0.0	7.220E-03	0.0	0.0	0.0	0.0	0.0
W-185	204	0	0	0	1.00	0.0	0.12	0.0	1.070E-07	0.0	0.0	0.0	0.0	0.0
W-187	205	0	0	0	1.00	0.0	0.24	0.0	8.060E-06	0.0	0.0	0.0	0.0	0.0

OUTPUT DATA

Post-accident temperature response of the core, T(°C) as a function of time, t(minutes), following a DBDA in the 1160 MW(e) HTGR

t	First Approximation of T	Second Approximation of T	Third Approximation of T
0	752	752	752
30	1071	1106	1106
60	1281	1363	1363
75	1370	1476	1476
90	1454	1581	1581
105	1532	1681	1681
120	1606	1777	1777
135	1677	1868	1868
150	1745	1955	1956
165	1811	2040	2040
180	1874	2122	2122
270	2220	2570	2570
360	2522	2967	2967
450	2797	3330	3331
540	3051	3670	3671
630	3289	3991	3992
720	3515	4297	4298
810	3730	4591	4593
900	3937	4875	4877
990	4136	5150	5152
1080	4329	5418	5420
1170	4516	5679	5681
1260	4698	5934	5936
1350	4875	6184	6186
1485	5133	6550	6552

APPENDIX B

DESIGN AND PERFORMANCE CHARACTERISTICS OF THE 1160 MW(e) HTGR CORE

REACTOR CORE DESIGN AND PERFORMANCE CHARACTERISTICS

Mechanical characteristics (dimensions at 72°F)

Fuel Element

Number required	3,944 (including 12 C's listed below)[a]
Shape	Hexagonal right prism
Material	Graphite
Width across flats (in.)	14.17
Length (in.)	31.22
Diameter of fuel holes (in.)	0.624
Number of interconnecting dowels	3

	Fuel Element	Control Fuel Element
Number of fuel holes	132	80
Number of coolant holes	72	43
Diameter of coolant holes (in.)	0.826 (6 are 0.717)	0.826 (10 are 0.717)
Number of burnable poison holes	6	—
Coolant channel flow area per element, nominal (ft^2)	0.262	0.151

Fuel Rods

Rod diameter (in.)	0.617
Fuel rod stack length (in.)	29.71
Rod composition	Bonded fissile and fertile particles in specified fuel compositions

[a] A = top keyed reflector and plenum elements; B = top control plenum elements; C = top region center reflector elements.

Hexagonal reflector elements	
Number required	3,267 (including 12 C's listed below)[a]
Shape	Hexagonal right prism
Material	Graphite
Width across flats (in.)	14.17
Length (in.)	31.22 (2,041 elements) 15.61 (1,129 elements) 23.41 (97 elements)
Coolant channel flow area in top and bottom reflector elements, nominal (ft^2)	0.325
Interconnecting dowels	3/element
Top reflector and plenum elements[a]	
Number required	607 total (522 A's; 73 B's; 12 C's)
Shape	Hexagonal right prism (A, B, C)
Material	Steel (A, B); graphite (C)
Width across flats (in.)	14.08 (A, B); 14.17 (C)
Length (in.)	15.61 (A); 23.41 (B, C)
Interconnecting dowels	3/element (A, B, C)
Core arrangement	
Pitch of fuel columns within refueling region (in.)	14.21
Number of fuel columns	493
Number of hexagonal side-reflector columns	114
Number of large side-reflector block columns	36
Number of control rod channels	146 (2 per fuel region)
Number of reserve shutdown channels	73 (1 per fuel region)

[a] A = top keyed reflector and plenum elements; B = top control plenum elements; C = top region center reflector elements.

Number of refueling regions	85 (73 in active core; 12 in reflector)
Refueling region pitch spacing (in.)	37.71
Effective active core diameter (ft.)	27.7
Active core height (ft.)	20.8
Equivalent side-reflector thickness, including shield (in.)	40.5
Top and bottom reflector thickness, each without core support (in.)	46.8
Lattice cell area (in.^{2})	175

Nuclear characteristics (initial core)

Core power density (kW/liter)	8.4
Core specific power (kW/kg U-235)	1,740

Average neutron flux (n/cm^2- sec)

	Fast (>0.18 MeV)	Thermal (<2.38 eV)
Beginning of cycle	5.08×10^{13}	1.05×10^{14}
End of cycle	5.15×10^{13}	1.32×10^{14}

C/Th ratio	214
C/U-235	4,350

Fuel loading (initial core)

Th (kg)	37,487
U (kg)	1,725

Average loading per fuel element

Th (kg)	9.5
U (kg)	0.44
U-235 enrichment (%)	93.15
Fuel element lifetime (yr.)	4
Average conversion ratio, initial core	0.68

Average burnup of U and Th (MWd/ton)	98,000
Fertile particle burnup (max)	7.5% FIMA
Fissile particle burnup (max)	78% FIMA
Control rod system worth, initial core	
Total worth, operating (Δk)	0.258
Maximum worth of one pair, operating (Δk)	0.015
Maximum worth of one pair, subcritical (Δk)	0.066
Nominal reserve shutdown system worth, initial core (Δk)	0.15
Prompt neutron lifetime, initial core, operating (sec)	4.1×10^{-4}

Thermal and hydraulic parameters at reactor design conditions

Gross reactor thermal power [MW(t)]	3,000
Total coolant flow at core exit (lb/hr)	10.936×10^6
Coolant inlet to core (°F)	639
Mixed-mean coolant temperature at core exit (°F)	1,392
Coolant channel frontal area fraction, core average, (%)	20
Total core coolant channel frontal flow area (ft^2)	121
Average fuel rod temperature (°F)	1,634
Average moderator temperature in active core (°F)	1,362
Average coolant channel surface heat flux (Btu/hr-ft^2)	66,000
Average coolant Reynolds number	59,000
Average coolant surface heat-transfer coefficient (Btu/hr-ft^2-°F)	285
Core inlet pressure (psia)	725

Total core pressure drop, maximum (psi)	11.5[b]
Volume of active core (ft^3)	12,500

Mass

Mass of standard graphite block (Kg)	82.1
Mass of fuel rods in standard element	Min. 31.7 to Max. 41.7
Total mass of standard fuel element assembly (Kg)	113.8 to 123.8
Total number of standard fuel elements in the core	3360
Mass of control graphite block (Kg)	80.3
Mass of fuel rods in control element (Kg)	Min. 16.3 to Max. 24.5
Total mass of a control fuel element (Kg)	96.6 to 104.8
Total number of control fuel elements in core	584

Fuel Mass

Average mass of uranium per fuel element (Kg)	0.44
Average mass of thorium per fuel element (Kg)	9.5
Average graphite per fuel element (Kg)	81.83

Fuel Temperature

Average fuel temperature	1634°F
Average graphite temperature	1362°F

[b] Includes drop of 1.5 psi across core support floor.

Reflector Elements

Number of hexagonal side reflector columns	114
Number of large side reflector blocks	36
Equivalent side reflector thickness	1028.7 mm
Equivalent top and bottom reflector thickness	1188.7 mm
Heat capacity of reflector	

VITA

Farzad Rahnema was born in Arak, Iran on December 26, 1950. He attended Bahman High School in Tehran from September 1963 to September 1968. In December 1974 he received the degree of Bachelor of Science in Engineering Mechanics from Illinois Institute of Technology and was admitted to the Institute's Graduate School. While pursuing his graduate studies, he was a research assistant in the Department of Mechanics, Mechanical, and Aerospace Engineering. In August 1975 he transferred to Louisiana State University in Baton Rouge where he is presently a candidate for the degree of Master of Science in the Department of Nuclear Engineering.

Farzad Rahnema is married to the former Mahnaz Ataii and is the father of one daughter, Nazgol, born on March 19, 1976. He is a student member of the American Nuclear Society.

EXAMINATION AND THESIS REPORT

Candidate: Farzad Rahnema

Major Field: Nuclear Engineering

Title of Thesis: High Temperature Gas Cooled Reactor Fuel Failure in the Absence of Core Cooling

Approved:

Robert E. Miles
Major Professor and Chairman

James B. Traynham
Dean of the Graduate School

EXAMINING COMMITTEE:

Frank A. Silady

John C Courtney

Robert C. McMillan

Robert E. Miles

Date of Examination:

April 13, 1977